Dual inhibitors of amyloid beta aggregation and sphingomyelin synthase from natural resources

(アミロイドβ凝集とスフィンゴミエリン合成酵素の二重阻害を示す天然資源化合物に関する研究)

A thesis

Submitted for the Degree of

Doctor of Life Science

Deepak H V

Laboratory of Molecular Chemical Biology

Transdisciplinary Life Science Course

Graduate School of Life Science

Hokkaido University, Japan

December 2020

Table of contents

Chapter-3: Daurichromenic Acid, a Novel Scaffold as Amyloid Beta Aggregation Inhibitor

Abbreviations

AD: Alzheimer's disease

APP: amyloid precursor protein

Aβ: Amyloid beta

Cdase: ceramidase

Cer: ceramide

CERK: ceramide kinase

CerS: ceramide synthase

$CHCl_3$: chloroform

DCA: daurichromenic acid

DCC: *N,N'*-Dicyclohexylcarbodiimide

DIEAP: *N,N*-Diisopropylethylamine

DMAP: 4-Dimethylaminopyridine

DMF: *N,N*-dimethylformamide

ER: endopasmic reticulam

ESIMS: electrospray ionization mass spectrometry

Et_3N: triethylamine

EtOAc: ethylacetate

GA: ginkgolic acid

GSL: glycosphingolipid

HIV: Human immune deficiency virus

IC_{50}: concentration for 50% inhibition of enzyme activity

LPP: lipid phosphate phosphatase

MeOH: methanol

MSHTS: microliter-scale high-throughput screening

NFT: neurofibrillary tangles

NMR: nuclear magnetic resonance

nSMase2: neutral sphingomyelinase 2

nM: nano molar

PD: Parkinson disease

Pd/C: palladium on carbon

PS: phosphotidylserine

QD: Quantum dot

QDAβ : Quantum dot amyloid beta

q: quartet

q: quintet

RD: *Rhododedron dauricum*

r.t: room temperature

SAR: structural activity relationship

SD: Standard deviation

s: singlet

SM: sphingomyelin

SL: sphingolipid

SMase: sphingomyelinase

SMS: sphingomyelin synthase

SMSr: sphingomyelin synthase related protein

SPHK: sphingosine kinase

S1P: sphingosine 1-phosphate

S1PRs: sphingosine 1-phosphate receptors

TBAF: tetra-*N*-butyl ammonium fluoride

TLC: thin layer chromatography

Chapter 1

Genera Introduction

1.1 Sphingolipids

Sphingolipids (SL) represent one of the major classes of eukaryotic lipids. Historically, the first sphingolipids were isolated from brain in the 1876 by Thudicum, who introduced the name 'sphingosine' after the Greek mythical creature, the Sphinx[1], because of their enigmatic nature. Biochemical and chemical approaches in the first part of the 20th century resulted in elucidation of the chemical structure of sphingosine, one of the major sphingoid bases, which are the founding blocks of all sphingolipids (distinguishing sphingolipids from other lipids). Sphingolipids are defined by the presence of a sphingoid base backbone, sphingosine. Sphingosine is (2*S*, 3*R*, 4*E*)-2-aminooctadec-4-ene-1,3-diol (it is also called D-*erythro*-sphingosine and sphing-4-enine).This discovery was followed by elucidation of the classes of complex sphingolipids (sphingomyelins and glycosphingolipids, including the gangliosides), which define the structural properties of membranes and lipoproteins and also have emerging roles in cell signaling, cell–cell interaction, cell recognition, and help to regulate cell growth and differentiation[2].

Sphingolipids are found in all animals, plants, and fungi, and in some prokaryotic organisms and viruses. They are composed of a sphingoid base backbone to which a fatty acid may be attached through an amide bond and a head group at the primary hydroxyl. The head groups range from a simple hydrogen to more complex species, such as the phosphocholine moiety of sphingomyelin (SM) and the simple to complex glycans of glycosphingolipids[3]. The hydrophobic and hydrophilic properties of sphingolipids made them amphipathic in nature. The main mammalian spingoid bases are dihydrosphingosine and sphingosine. Sphingomyelin, a component not found in plants, and some neutral and acidic

glycolipids as complementary constituents to phosphoglycerolipids and cholesterol in the plasma membrane structure.

Sphingolipids are synthesized in a pathway that begins in endoplasmic reticulum (ER) and completed in the Golgi apparatus, but these sphingolipids are enriched in plasma membrane and in endosomes, where they perform their function[4]. They have a significant role in plasma membrane and as modulators of cell–cell interactions and in cell recognition. Also responsible for cell cycle arrest, apoptosis, senescence, immunity, autophagy, migration and differentiation. With these roles, sphingolipids and sphingolipid synthesis emerge as a logical target for drug development, with the common of the thus-far tested drugs targeting enzymes that are involved in the production of various sphingolipid subtypes[5].

Sphingolipid structures differ significantly from kingdom to kingdom and sphingolipid diversity within the animal kingdom itself has been recognized. General structure of sphingolipids are as follows (Figure 1).

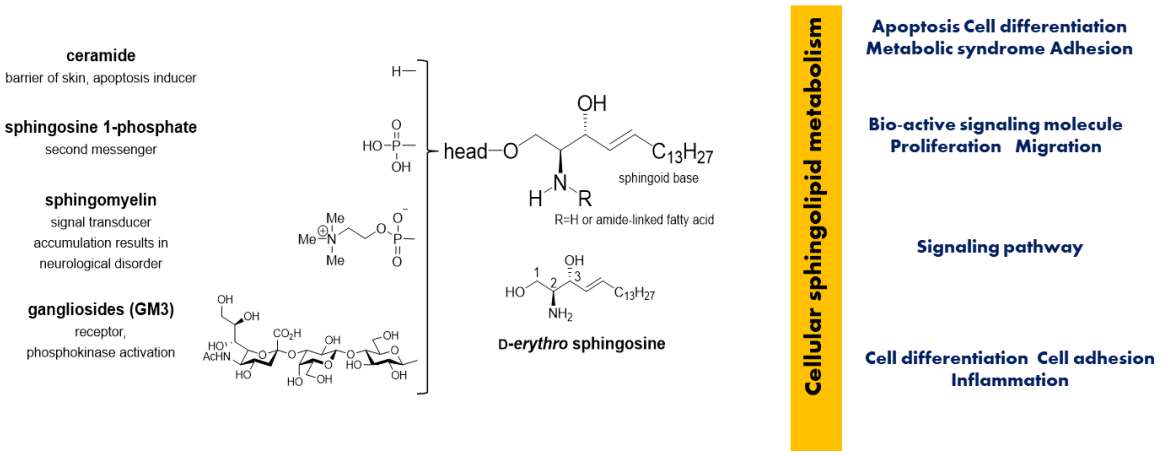

Figure 1: General structure of sphingolipids and functions

1.2 Sphingolipid metabolism and its biosynthetic pathways

The central metabolite of sphingolipid metabolism is ceramide. Ceramide is a class of molecules rather than a single molecule, which serves as the structural and metabolic precursor for complex sphingolipids and contains amide-linked acyl chains of different lengths[6] (Figure 2).

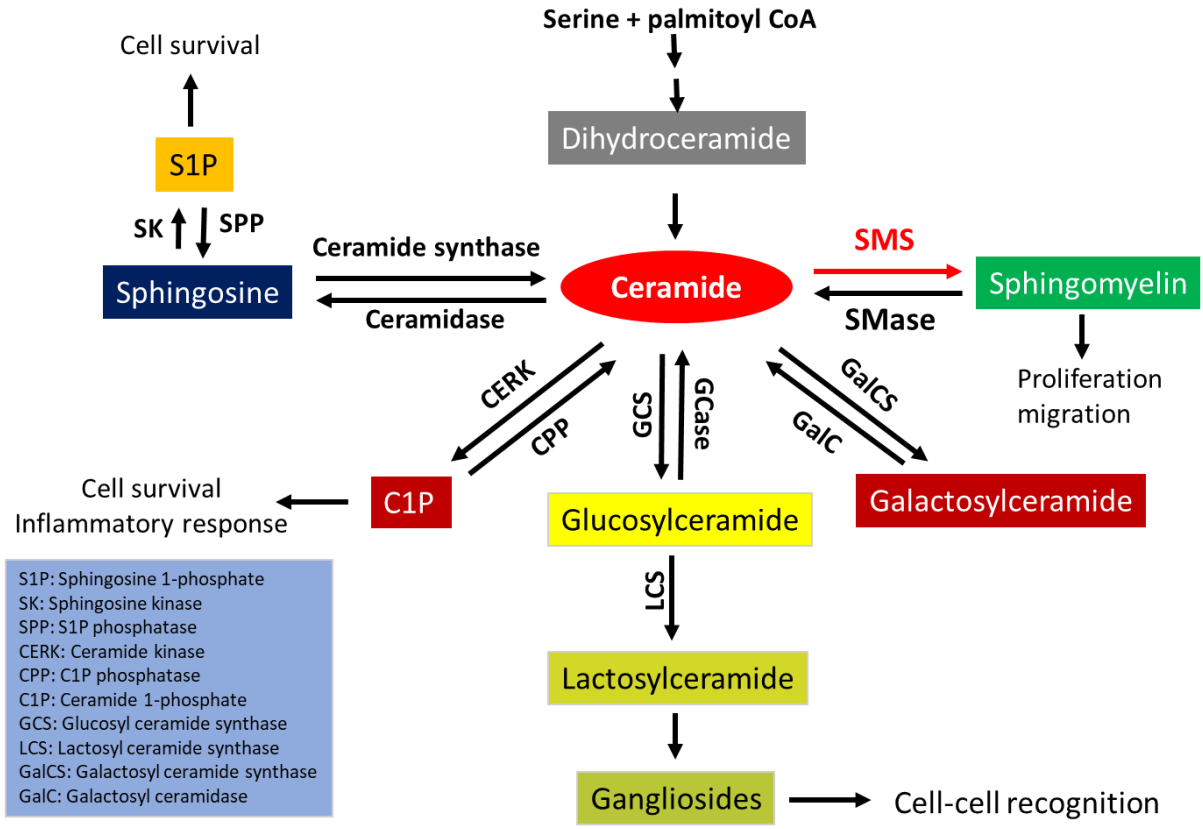

Figure 2: Sphingolipid metabolism and important biochemical pathways.

More than 200 subspecies of mammalian ceramides are the result of combinatorial synthesis from collaboration of several enzymes[7]. Ceramides of different chain lengths may have opposing effects in different tissues[8]. They can be synthesized de novo in the endoplasmic reticulum by the condensation of serine and palmitoyl-Co A by the action of serine palmitoyl transferase, followed by the sequential act of 3-ketodihydrosphingosine reductase, (dihydro) ceramide

synthases (CerS) and dihydroceramide desaturase (Des) (Fig 2). The last step of the de novo ceramide synthesis pathway is the oxidation of dihydroceramide (dhCer) to ceramide by dihydroceramide desaturase 1[9]. Physiological and pathological functions of ceramide are well known. Cer has been implicated in variety of physiological functions including apoptosis, cell growth arrest, differentiation, cell senescence, cell migration and adhesion. Chemical and genetic suppression of Des led to dhCer accumulation, which led to apoptosis, cell cycle arrest, and autophagy[9]. In the plasma membrane and lysosomes complex sphingolipids are broken down into sphingosine, which can be recycled back by CerS to ceramide[10]. Possible enzymes taking part in this pathway are ceramidases, dihydro ceramide synthases and SMases. Ceramides can be glycosylated by glucosylceramide synthase (GCS) to produce glucosylceramide, which is linked to multi-drug resistance or deacylated by ceramidase to form sphingosine, which shows anti-tumor activity[11]. Metabolism of ceramide to sphingomyelin and to most complex glycosphingolipids occurs in the golgi. Transportation of ceramide from endoplasmic reticulum (ER) to golgi is mediated by the ceramide transfer (CerT) protein during sphingomyelin synthesis and by vesicular transportation during glycospingolipid synthesis[12]. Sphingosine can further be phosphorylated to S1P by the catalytic activity of sphingosine kinases. S1P promotes angiogenesis, cancer cell proliferation and metastasis [13]. Ceramides can also be phosphorylated in the trans-golgi and possibly in the plasma membrane to produce ceramide 1-phosphate by ceramide kinase (CK). Sphingolipids have rapid turnover and their levels are maintained by the balance between synthesis and degradation in different compartments [13]. (Figure 2) Sphingolipid metabolism pathways Sphingolipids are inter-convertible and ceramide is the central molecule of sphingolipid metabolism. It can be synthesized de novo by the condensation of serine and palmitoyl CoA or

from the hydrolysis of sphingomyelin or cerebrosides (Glucosylceramide, Galactosyl ceramide).

1.3 Sphingomyelin synthase (SMS)

Sphingomyelin synthase (SMS) , an enzyme which catalyzes the conversion of ceramide and phosphatidylcholine to Sphingimyelin (SM) and diacylglycerol (Figure 3) SMS is a cell membrane-located lipid-metabolizing enzyme, which has been reported to play crucial roles in cell death, proliferation, and migration.

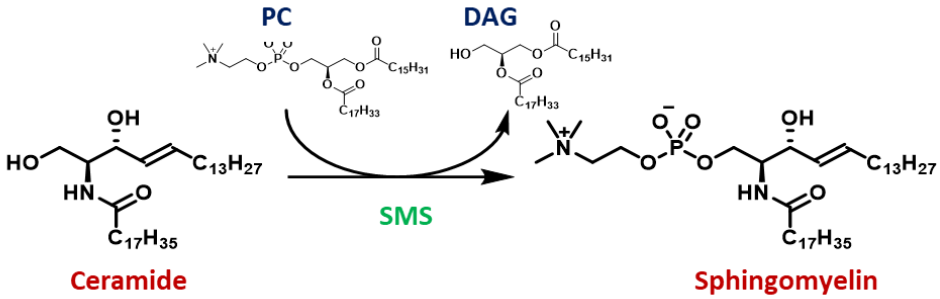

Figure 3: Conversion of ceramide to sphingomyelin by SMS

SMS has three isoforms: SMS1 SMS2 and SMSr. Although both enzymes catalyze the same reactions, their subcellular localizations are different: SMS1 is found in the trans-Golgi apparatus, while SMS2 is predominantly found in the plasma membranes. SMSr is localized in endoplasmic reticulum (ER) which is a suppressor of ceramide-induced mitochondrial apoptosis.

The sequences of SMS1 and SMS2 suggest that they are integral membrane proteins with multiple membrane-spanning core domains (Figure 4). Localization of SMS isoforms and their similarities and domain architecture of SMS. SMS1 and SMSr control the ceramide homeostasis in Golgi apparatus and endoplasmic reticulum respectively. The membrane protein, SMS2 associated with metabolic disorder such as obesity, diabetes, atherosclerosis etc[14]. SMS2

activity also responsible for the generation of amyloid-beta peptide[15], HIV-1 envelop-mediated membrane fusion and induction of colitis-associated colon cancer[16]. Thus, SMS2 could be a potential therapeutic target for these diseases.

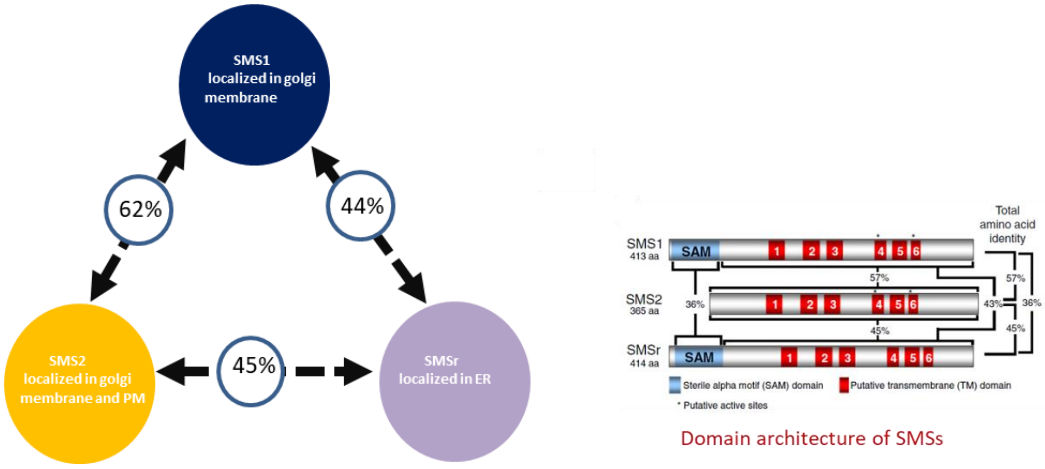

Figure 4: Localization of SMS and Domain structure of SMSs

SMS1, SMS2, and SMSr have six transmembrane (TM) domains and their N- and C-termini are facing cytosol. In SMS1 and SMSr, there is a sterile alpha motif (SAM) at N-terminus. The SAM domain may play a role in cellular functions such as development, signal transduction, and transcriptional regulation through protein–protein or protein–lipid interaction.[2] The proteins, which interact with SAM domain of SMS1, have not identified, and SAM domain function is unclear.

1.4 SMS allied disorders

Sphingomyelin synthase (SMS) sits at crossroads sphingolipid biosynthesis. Blockage of SMS activity should influence not only SM and ceramide levels, but also those of related sphingolipids, including glycosphingolipid, sphingosine, and S1P. Sphingomyelin synthase (SMS) is a cell membrane-located lipid-metabolizing enzyme, which has been reported to play crucial roles in cell death,

proliferation, and migration[16].SMS also play key role in metabolic diseases and alzheimer's by clearance of Aβ .

Amyloid beta peptide (Aβ) is produced through the proteolytic processing of a transmembrane protein, amyloid precursor protein (APP), by β- and γ-secretases (Figure 5). Aβ accumulation in the brain is proposed to be an early toxic event in the pathogenesis of Alzheimer's disease, which is the most common form of dementia associated with plaques and tangles in the brain. The Aβ peptides are cleaved from the much larger precursor APP. APP is an integral membrane protein expressed in many tissues, especially in the synapses of neurons, which plays a central role in Alzheimer's disease (AD) pathogenesis. APP is best known as the precursor molecule cut by β-secretases and γ-secretases to produce a 37 to 49 amino acid residue peptide, Aβ. Recent studies have demonstrated that the extracellular Aβ is associated with exosomes, small membrane vesicles of endosomal origin. The fate of Aβ in association with exosome is largely unknown.

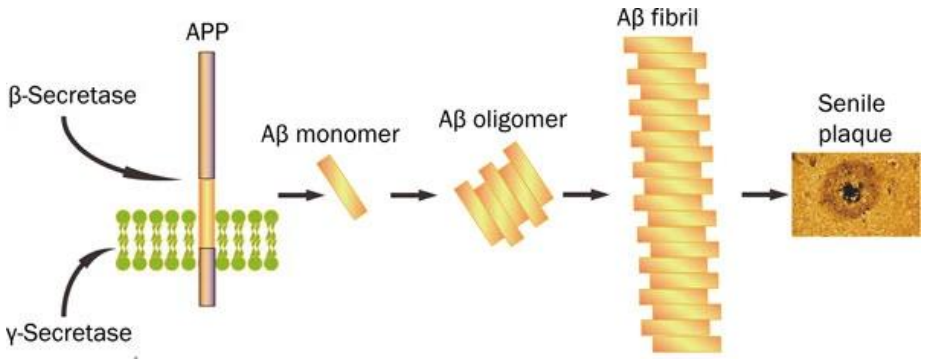

Figure 5: Cleavage of β-secretases and γ-secretases by APP

Recently K. Yuyama et.al recently demonstratedthe secretion of neuronal exosomes is modulated by the activities of sphingolipid metabolizing enzymes, neutral sphingomyelinase 2 (nSMase2) and SMS2. Up-regulation of exosome secretion from neuronal cells by treatment of SMS2 siRNA enhanced Aβ

(pathogenic agent of Alzheimer disease) uptake into microglial cells and significantly decreased extracellular levels of Aβ (Figure 6).

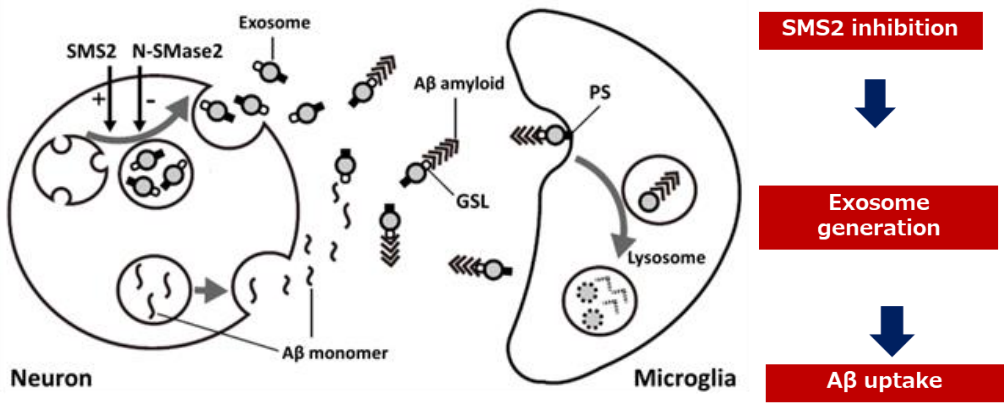

Figure 6: Inhibition of SMS 2 to production of exosomes

New finding indicates a novel mechanism responsible for clearance of Aβ through its association with exosomes. The potent and selective SMS2 inhibitors are well in need to modulate exosome production by the inhibition of SMS2 in neuronal cells. This strategy will be a way to identify a small molecule drug for the treatment of Alzheimer's disease.

The elevation of Aβ generation is also associated with the increase in SMS activity.[15] The SMS is significantly expressed in AD brain especially in hippocampus not in cerebellum. To understand the role of SMS in AD, CHO-APP cells were treated with the SMS inhibitor D609, as a result there is dose and time dependent decrease in Aβ deposition (Figure 7). The decrease in Aβ level occurred without changes in APP expression or cell viability.

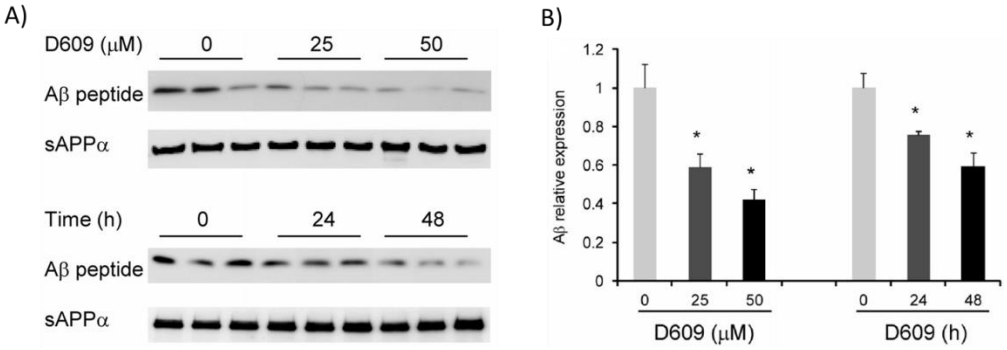

Figure 7: Impact on Aβ generation by SMS inhibition A) time and dose dependent treatment of D609 on CHO-APP cells and measurement of Aβ deposition B) quantification data

Ceramide is known to be apoptosis inducer sphingolipid and ceramide accumulation has been found during chemotherapy. A lower level of ceramide with higher activities of GCS and SMS was detected in drug resistant human leukemia 60 (HL-60) cells than IN HL-60 cells. It has been observed lower level of ceramide in case of chemo resistant leukemia patients that chemo sensitive patients. The GCS and SMS activity are two-fold higher in case of chemo resistant HL-60 cells[17] (Figure 8). These results suggest that the apoptotic mechanism of drug resistant leukemia patients regulated ceramide content, GCS and SMS activity.

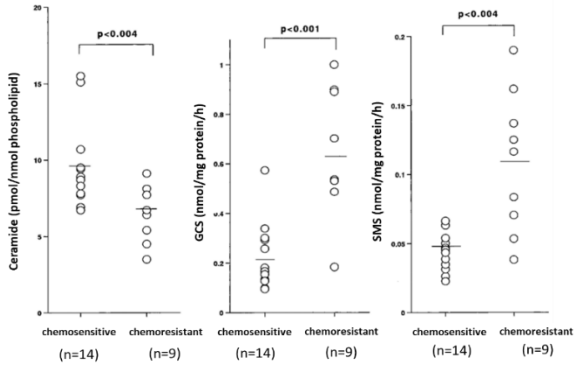

Figure 8: ceramide level, GCS and SMS activity in chemo sensitive and chemo resistant HL-60 cells

The role of sphingolipids and sphingolipid metabolizing enzymes in metabolic disorders are being known. Many studies suggest that the abnormalities of sphingolipid metabolism may be involved in inflammation and carcinogenesis.[18] (Figure 9) shows activity of SMS in knockout mouse and in inducing fat deposition in liver and (B) shows comparison of wild type and knockout mouse with SMS and to report TG level in liver

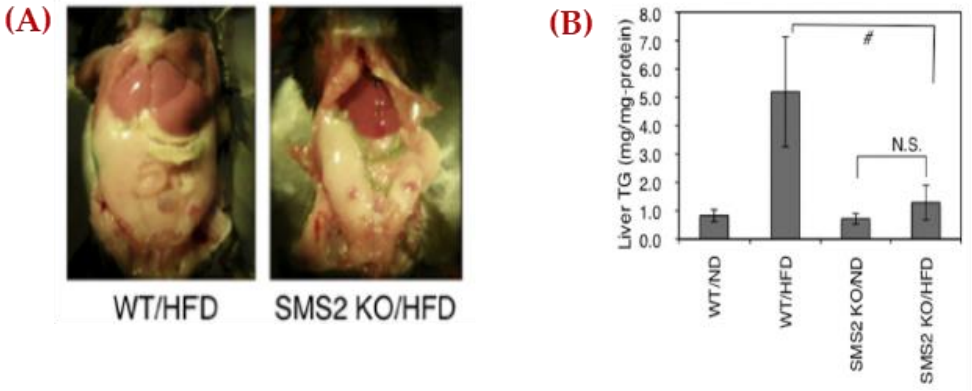

Figure 9 (A) SMS KO studies of high fat diet induced mouse in liver (B)TG level in liver

Very recent study colon cancer and sphingolipid metabolizing enzyme reports SMS2 deficiency inhibits DSS (dextran sodium sulfate)-induced colitis and subsequent colitis-associated colon cancer via inhibition of colon epithelial cell–mediated inflammation.[19] The increase in ceramide or decrease in SM or both plays a role in the suppression of colon inflammation and colitis-associated colon cancer need to be clarified. The effect of SMS1 on colon inflammation and colitis-associated colon cancer is not known.

1.5 References

1. Hannun YA, Obeid LM. Sphingolipids and their metabolism in physiology and disease *Nat Rev Mol Cell Biol*. 2018, 19, 175-191.

2. Adada M, Canals D, Hannun YA, Obeid LM. Sphingolipid regulation of ezrin, radixin, and moesin proteins family: implications for cell dynamics. *Biochim Biophys Acta*. 2014, 1841, 727-737.

3. Merrill, A. H. & Sandhoff, K. *Biochemistry of Lipids, Lipoproteins and Membranes, 4th edition*. *New Comprehensive Biochemistry* (2002).

4. Futerman, A. H. Intracellular trafficking of sphingolipids: Relationship to biosynthesis. *Biochimica et Biophysica Acta - Biomembranes* (2006).

5. Cuperlovic-Culf, M. *NMR metabolomics in cancer research*. *NMR Metabolomics in Cancer Research* (2012).

6. Gault CR, Obeid LM, Hannun YA. An overview of sphingolipid metabolism: from synthesis to breakdown. *Adv Exp Med Biol*. 2010, 688, 1-23.

7. Hannun YA, Obeid LM. Many ceramides. *J Biol Chem*. 2011, 286, 27855-27862.

8. Ponnusamy S, Meyers-Needham M, Senkal CE, et al. Sphingolipids and cancer: ceramide and sphingosine-1-phosphate in the regulation of cell death and drug resistance. *Future Oncol*. 2010, 6, 1603-1624.

9. M. Casasampere, Y.F. Ordonez, A. Pou, J. Casas, Inhibitors of dihydroceramide desaturase 1: Therapeutic agents and pharmacological tools to decipher the role of dihydroceramides in cell biology, *Chemistry and physics of lipids*, 2016 197, 33-44

10. Kitatani, J. Idkowiak-Baldys, Y.A. Hannun, The sphingolipid salvage pathway in ceramide metabolism and signaling, *Cellular signalling*, 2008, 20, 1010-1018.

11. B.J. Pettus, C.E. Chalfant, Y.A. Hannun, Ceramide in apoptosis: an overview and current perspectives, *Biochim Biophys Acta*, 2002, 1585, 114-125.

12. M. Maceyka, S. Spiegel, Sphingolipid metabolites in inflammatory disease, *Nature*, 2014 510, 58-67.

13. S.A. Saddoughi, P. Song, B. Ogretmen, Roles of bioactive sphingolipids in cancer biology and therapeutics, *Sub-cellular biochemistry*, 2008, 49, 413-440.

14. H. Hanamatsu, S. Ohnishi, S. Sakai, K. Yuyama, S. Mitsutake, H. Takeda, S. Hashino, Y. Igarashi, *Nutr. Diabetes*, 2014, 4, e141

15. Hsiao JH, Fu Y, Hill AF, Halliday GM, Kim WS. Elevation in sphingomyelin synthase activity is associated with increases in amyloid-beta peptide generation. *PLoS One*. 2013, 8, e74016.

16. Tafesse, F.G.; Huitema, K.; Hermansson, M.; Van Der Poel, S.; Van Den Dikkenberg, J.; Uphoff, A.; Somerharju, P.; Holthuis, J.C.M. Both sphingomyelin synthases SMS1 and SMS2 are required for sphingomyelin homeostasis and growth in human HeLa cells. *J. Biol. Chem.* 2007, 282, 17537–17547.

17. Itoh, M., Kitano, T., Watanabe, M., Kondo, T., Yabu, T., Taguchi, Y., Iwai, K., Tashima, M., Uchiyama, T., & Okazaki, T. Possible role of ceramide as an indicator of chemoresistance: decrease of the ceramide content via activation of glucosylceramide synthase and sphingomyelin synthase in chemoresistant leukemia. *Clinical cancer research,* 2003, *9*, 415–423.

18. Furuya, H., Shimizu, Y., & Kawamori, T. Sphingolipids in cancer. *Cancer metastasis reviews*, 2011, *30*, 567–576.

19. Ohnishi, T., Hashizume, C., Taniguchi, M., Furumoto, H., Han, J., Gao, R., Kinami, S., Kosaka, T., & Okazaki, T. Sphingomyelin synthase 2 deficiency inhibits the induction of murine colitis-associated colon cancer. *FASEB*, 2017, *31*, 3816–3830.

Chapter-2

Daurichromenic acid and its derivative (-) hongoquercin A

New scaffold and potential targets for sphingomyelin synthase inhibition

2.1 Abstract

Sphingomyelin synthase (SMS) is a key enzyme to biosynthesize sphingomyelin that regulates membrane fluidity and microdomain structure. SMS plays crucial roles in mediating metabolic syndrome tumorigenesis and Alzheimer's disease. Thus, SMS could serve as a potential therapeutic target for many diseases. However, few SMS inhibitors were reported. In this paper we focused on discovery of new scaffold small molecule inhibitor or natural plant extracts with high potential value. To identify potential therapeutic agents, we screened methanol extracts derived from 650 Japanese medical plants for their sphingomyelin synthase activity by using invitro assay. Of these extracts, the leaves of *Rhododendron dauricum* was the most active in inhibiting sphingomyelin synthase inhibition. Bioguided fractionation of *Rhododendron dauricum* leaves lead to isolate a new scaffold potent SMS inhibitor, a meroterpenoid daurichromenic acid with IC_{50} value of 7 μM for SMS1 and 4 μM SMS2. This is a first report on daurichromenic acid which detailed about inhibition of sphingomyelin synthase, so apart from isolation we have also synthesized series of daurichromenic acid derivatives to evaluate its SAR studies. Structural activity relationship validation of DA helped us to understand the role of functional group against SMS activity. Among derivatives compound 7 and unnatural Hongoquercin were found to be potent SMS inhibitor which reveal carboxylic acid group participation is very important to keep its inhibition activity. Discovery of Daurichromenic acid and synthesizes (-) hongoquercin A as a novel class of SMS inhibitors would advance in future discovery of potential SMS inhibitors.

2.2 Introduction

Sphingomyelin synthase (SMS), an enzyme which catalyzes the conversion of ceramide and phosphatidylcholine to Sphingomyelin (SM) and diacylglycerol. (Figure 1) Sphingomyelin synthase has three isoforms SMS1, SMS2 and SMSr. SMS1 and SMSr control the ceramide homeostasis in Golgi apparatus and endoplasmic reticulum respectively. The membrane protein, SMS2 associated with metabolic disorder such as obesity, diabetes, atherosclerosis and has significant role in maintaining cell homeostasis.[1] where as SMSr is localized in endoplasmic reticulum (ER) which is a suppressor of ceramide-induced mitochondrial apoptosis.[2] In a recent report, the deficiency of plasma membrane protein SMS2 attenuates the development of *obesity*, fatty liver and type 2 diabetes.[3] The SMS2 activity has been involved in other metabolic disorders such as insulin resistance.[4] SMS2 activity also associated with the generation of amyloid-beta peptide[5] HIV-1 envelop-mediated membrane fusion[6] and induction of colitis-associated colon cancer.[7] Thus, SMS2 is expected to be potential target for the treatment of many diseases.

Modulation of the activity of a specific enzyme or receptor by a small molecule is one of the cornerstones of modern target-based drug discovery. However, small molecules frequently bind to multiple target molecules, influencing both drug efficacy and safety[8]. To understand SMS biology in disease condition we need potent and selective SMS inhibitors. Natural products have been emerging as source of potential drug candidates since few decades.[9] However, the model inhibitor of SMS from natural resources has not been discovered at all. Identification of inhibitors from natural resources to target molecules involved in human diseases is a big and attractive challenge in the field of chemical biology,

because natural products have been had good track record in application of drug discovery.

So far, few small molecule inhibitors are reported. Ginkgolic acid is the first known natural SMS inhibitor which was originally identified from our group. Unfortunately, it is not practically useful because of its toxicity. In search of new small molecule with high potency and stability X.[10]also we find out melborones which inhibits sms2 and diabetic deficiency and which also a natural product.[11] We explore Hokkaido plants in search of potent SMS inhibitor. Here, we identified and isolated a natural SMS inhibitor daurichromenic acid (DA), from *Rhododendron dauricum.* Its meroterpenoid composed of orsellinic acid and sesquiterpene moieties [12]. DCA has attracted considerable attention because it displays various interesting pharmacological activities Especially, DCA has been one of the most effective natural products with anti-HIV properties, as shown in experiments with acutely infected H9 cells, in which the EC50 value of DCA (15 nM) was smaller than that of the positive control drug azidothymidine (44 nM)[13] Thus, DCA has been extensively studied over the past few years and we here isolated, synthesized its derivatives and confirmed its structure-activity relationship (SAR) study toward SMS.

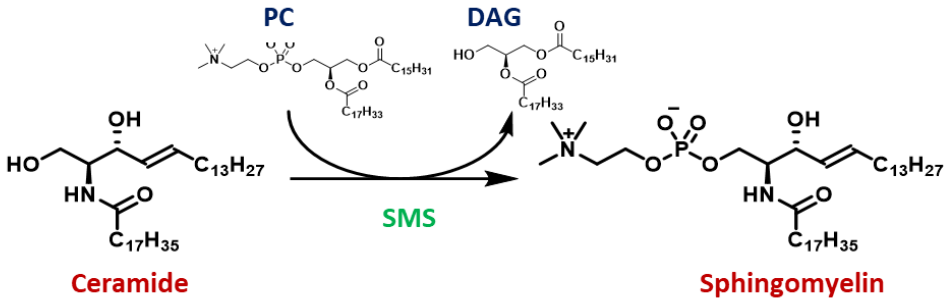

Figure 1: Conversion of ceramide to sphingomyelin through SMS pathway

The plant *Rhododendron dauricum* (Ericaceae) is distributed in China, Siberia and north part of Hokkaido. Dried leaves of *Rhododendron dauricum* known as Manshanfong have been used in Chinese herbal medicine to treat many diseases such as acute-chronic bronchitis and as expectorant[14.] MeOH extracts of leaves of this plant which shows significant Anti-HIV activities[15]. As while exact nature of active components are still unknown, Chinese traditional herbal medicines have been practiced from many years for their vast clinical treatment of disease. However, the active principles responsible for sphingomyelin synthase inhibition of *Rhododendron dauricum* have not been identified.

Taken together, drugs with the potential sphingomyelin synthase inhibition are in demand. In this connection we screened 650 medicinal plant extracts which were grown wildly or cultivated in Hokkaido, Japan, to ascertain their activity against sphingomyelin synthase inhibition. Inhibition activity was evaluated by invitro SMS assay. Using this screening method, *Rhododendron dauricum* L. (RD, Ericaceae) was chosen for further investigation because the dried leaves are used as crude drug having various biological activities and its availability from private gardens, but anti-SMS activity is still unknown. In this connection bio-guided isolation lead to isolate daurichromenic acid from the dried leaves, a new scaffold inhibitor SMS inhibition. Apart from isolation we also focused on SAR studies of its synthesized three derivatives which may lead to develop new drugs for many metabolic syndrome tumorigenesis and AD.

2.2 Result and Discussion

2.2.1 Bioassay-Guided Isolation of Daurichromenic acid from R. *dauricum*

Recently we isolated ginkgolic acid from *Ginkgo biloba* (Family: Ginkgoaceae) from our plant library extracts and it regarded as one of the strong and first natural product inhibitors for sphingomyelin synthase inhibition[10]. To extend our

studies and to intend to search for novel scaffold inhibitor for SMS, the invitro assay method is used to screen 650 Hokkaido plant extracts to identify novel SMS1 and SMS2 inhibitors. A well-known Chinese crude medicine *Rhododendron dauricum* (RD) was chosen based on SMS assay results and its bioavailability for further Daurichromenic acid (DA, EC_{50}: SMS1 :7 µM, SMS2: 4 µM) a meroterpenoid, was isolated from ether soluble fraction of methanolic extract of the fresh leaves of R. *dauricum* (Family: Ericaceae) by repeated chromatographic separation and purification over silica gel (Figure 2). Structure was confirmed by ^{1}H, ^{13}C NMR and ESI-MS data analysis as well as compared with previously reported values.[16] ESI-MS showed m/z (M+1-18) = 353.46, suggesting the molecular formula of isolated compound $C_{23}H_{30}O_4$

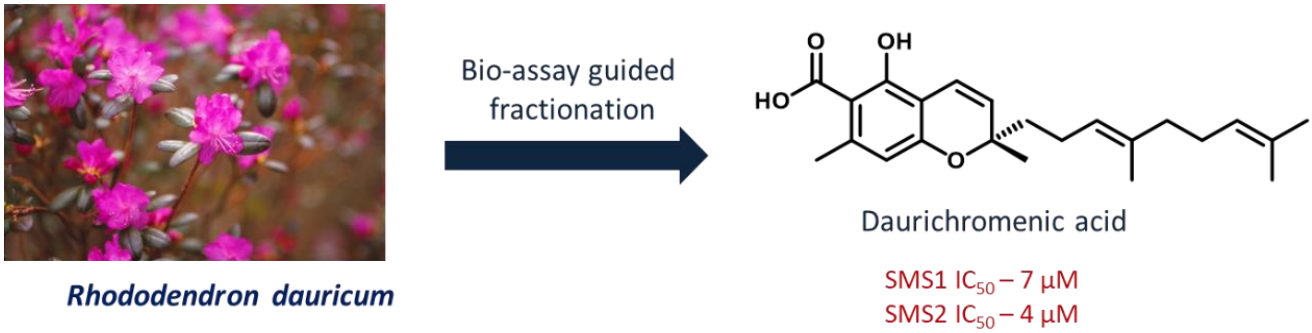

Figure 2: Isolation of DCA from Rhododendron dauricum and Inhibition activity of daurichromenic acid with IC50 of 7 µM on SMS1 and 4 µM on SMS2. IC_{50} values were measured by cell-based assay system: SMS expressing cell lysates (20 mM tris-buffer, 100 mL) and compounds were incubated for 3 hours at 37°C, then fluorescent lipids were extracted from lysates by the Bligh-Dyer method, and directly applied to HPLC.

2.2.2 Synthesis of daurichromenic acid derivatives and (-) hongoquercin A

The identity of DCA (**1**) isolated from *Rhododendron dauricum* was confirmed by ^{1}H- and ^{13}C-nuclear magnetic resonance (NMR) and by electrospray ionization-

mass spectrometry (ESI-MS) and compared with previously reported values[13]. To understand the structure–activity relationship (SAR) between DCA and its target molecules, DCA derivatives were synthesized. Compound (**2**) was prepared from DCA by selective methyl esterification of its carboxylic acid moiety by TMS-CH_2N_2. Compound (**3**) was prepared by protecting the carboxylic acid and hydroxy groups with iodomethane, and compound (**4**) was prepared by hydrolysis of the methyl ester group of compounds (**3**). Subsequently, hongoquercin A (**7**), which has been isolated from an unidentified terrestrial fungus[16] and exhibits antibacterial properties toward methicillin-resistant *Staphylococcus aureus* and vancomycin-resistant *Enterococcus faecium*[17,18], was prepared from compound (**2**). In the first step, compound (**2**) was treated with $FeCl_3$ to obtain the cyclized derivative compound 5 (**5**). The methyl ester group of (**5**) was hydrolyzed to yield compound (**6**), and the double bond at the benzyl position of compound (**6**) was reduced by Pd/C and H_2 to obtain (-) hongoquercin A (**7**) in moderate yield (Figure 3)

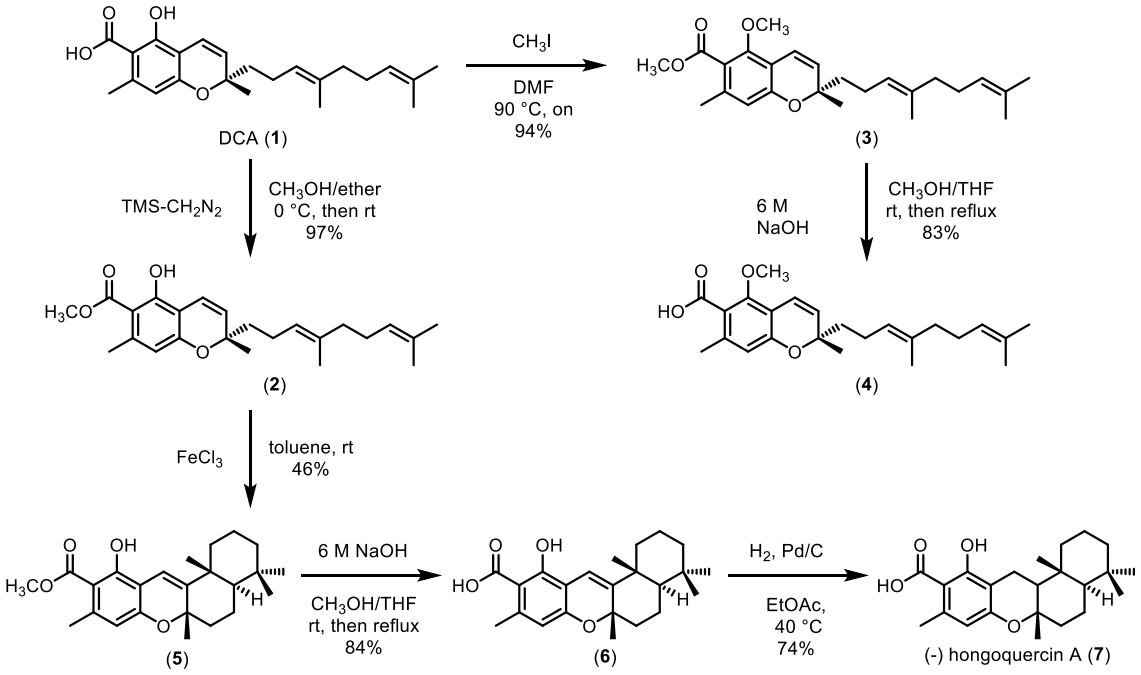

Figure 3: Synthesis of DCA derivatives

2.4 SAR studies of daurichromenic acid and their all derivatives

The ability of DCA and its derivatives to inhibit the SMS isozymes SMS1 and SMS2 was evaluated using a cell lysate assay and the fluorescent substrate C6-NBD (4-nitrobenzo-2-oxa-1,3-diazole)-Cer. DCA (**1**) and compounds **4**, **6**, and **7** showed relatively moderate inhibitory activities, with IC_{50} values of 7, 17, 9, and 4 μM, respectively, for SMS1, and 4, 10, 7, and 5 μM, respectively, for SMS2 (Figure 4).

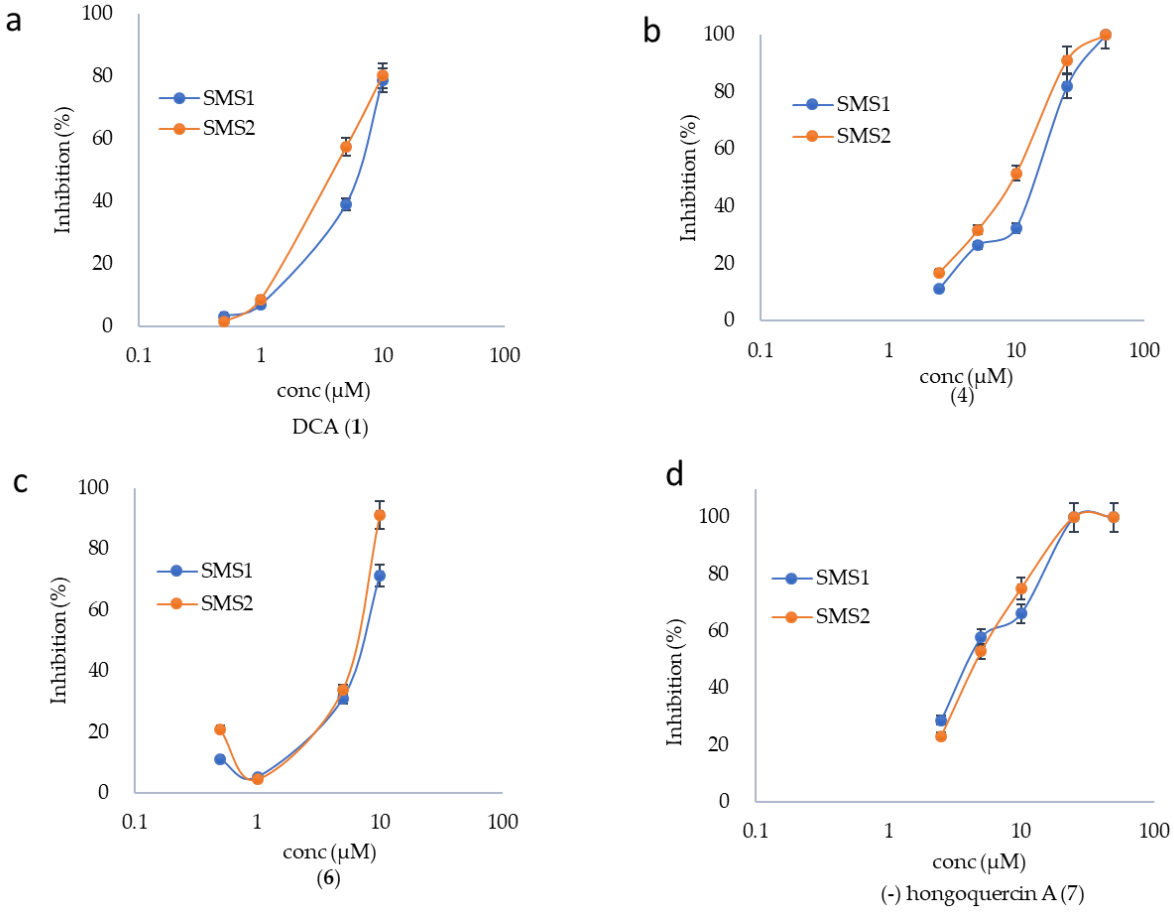

Figure 4. Inhibition of SMS1 and SMS2 activities by (**a**) DCA (**1**), (**b**) derivative (**4**), (**c**) derivative (**6**) and (**d**) derivative (**7**). IC_{50} values were measured using a cell lysate assay. SMS-expressing cell lysates and compounds were incubated for

3 h at 37 °C, and the extracted fluorescent lipids were directly analyzed by HPLC. Each point represents the mean ± SD of triplicate assays.

like other natural compounds [10, 11]. These findings indicated that the methyl esters of DCA derivatives, compounds **2**, **3**, and **5**, were inactive in these assays. Thus, the carboxylic acid group of DCAs are essential moieties for their inhibition of SMSs. Inhibitory activities of DCA, its derivatives, on natural sphingomyelin synthase towards SMS inhibition and their IC_{50} (Table 1) However, the SMS has not been succeeded in its crystallization. Therefore, a direct comparison with the previously isolated SMS inhibitor ginkgolic acid [10] has been examined. The chemical similarity of ginkogolic acid to DCA, as it is a long alkyl chain and a carboxylic acid moiety in an aromatic ring, shows that these two inhibitors also have the same functional group participation to inhibit SMS.

Compounds	SMS assay (SMS1)	SMS assay (SMS2)
	(IC_{50} in µM)	(IC_{50} in µM)
1	7	4
4	17	10
6	9	7
7	4	5

Table 1. Inhibitory activities of DCA, its derivatives, on natural sphingomyelin synthase towards SMS inhibition and their IC_{50}

Statistical analysis was performed using excel and Log [inhibitor concentration] vs activity was used for curve adjustment model for IC_{50} measurement Inhibition activities of daurichromenic acid and its derivatives 1-7 on SMS1 and SMS2. IC_{50} values were measured by cell-based assay system: SMS expressing cell lysates (20 mM tris-buffer, 100 mL) and compounds were incubated for 3 hours at 37°C,

then fluorescent lipids were extracted from lysates by the Bligh-Dyer method, and directly applied to HPLC.

We performed SMS assay of all intermediates during (-) hongoquercin A synthesis, we obtained compound 6 and 7 as potent SMS inhibitors. Collectively, from SAR study of DA, we obtained compounds 1, 4, 6 and 7 as potent SMS inhibitors. In future these SMS inhibitors need to be explored in cell-based assays and to address their efficacy in metabolic disorders and Alzheimer's disease.

2.4 Experimental section

2.4.1 Materials and Methods

^{1}H-NMR, ^{13}C spectra were recorded on a Varian Inova instrument (500 MHz) at 25°C in $CDCl_3$, and CD_3OD using TMS as internal standard. Chemical shifts (δ) are reported in parts per million and coupling constant values (*J*) are reported in Hertz (Hz). NMR solvents, $CDCl_3$, and CD_3OD were purchased from Cambridge Isotope Laboratories (Tewksbury, MA). Chemical shifts (δ) are reported in ppm and coupling constant values (J) are in Hertz (Hz) relative to CDCl3 (1H, δ 7.26; 13C, δ 77.00) or CD3OD (1H, δ 3.4, 4.8; 13C, δ 49.3) and tetramethyl silane. The following abbreviations were used for signal multiplicities: s = singlet; d = doublet; t = triplet; q = quartet; m = multiplet. All the other solvents used were of reagent grade and were purchased from Kanto Chemical (Tokyo, Japan). ESI-MS spectra were recorded on a JEOL JMS-T100LP spectrometer. Melting points were measured on a Micro Melting Point Apparatus, (Yanaco Co., Ltd). Analytical TLC was performed on 0.2 mm silica gel plates (Merck 60 F-254). Silica gel for column chromatography (Kanto Silica Gel 60, spherical, 40–50 μm). TLC plates: Silica gel 60 F_{254} (Merck), developed with $CHCl_3$: MeOH: H_2O (65:35:10, lower phase), sprayed with a mixture of 5%

ammonium molybdate and 1% cerium (IV) sulphate in 3.6N H_2SO_4 (Hanessian stain solution), or detected with UV lamp (UVGL-58 handheld at 254 nm).

2.4.2 Construction of plant extracts library

To construct plants extracts library, approximately 650 plants grown wildly or cultivated in Hokkaido area were collected. Each plant was dried by hot air at 50°C for 24 hours. Dried plants were cut into small pieces/powdered by grinder. Each dried plant (20 g) were extracted with 200 ml of MeOH at room temperature for 1 day. The MeOH solutions were filtered and concentrated in vacuo to dryness. Each of residues and the solutions dissolved in DMSO at the concentrations of 100 mg/ml were stocked at -20°C respectively

2.4.3 Plant collection

Leaves of *Rhododendron dauricum* was cultivated in Sapporo at its north area and were collected in September 9, 2015. The fresh leaves were dried by hot air at 50℃ for 24h.

2.4.4 Extraction and Isolation of active principle from Rhododendron dauricum

Leaves of Rhododendron dauricum was collected from Hokkaido, Japan were dried and powdered well (81 g). The dried powder was extracted with methanol (400 mL x 3) at room temperature three times after 24 hours each. The combined MeOH extract was concentrated under reduced pressure to give a black residue (24.2 g), which was dissolved in 20% MeOH in water (500 mL) and partitioned with hexane (200 mL x 3) Et2O (200 mL x 3) and EtOAc (200 mL x 3). After removal of solvent by evaporation, the hexane, Et2O, EtOAc and water residues were used for SMS assay. We found that hexane fraction was active than Et_2O fraction but, EtOAc and water fractions turned out to be inactive. The active Hexane fraction (3.8 g) was further fractionated and sub-fractionated by silica gel

column chromatography guided by bioassay. The active component was identified as daurichromenic acid, which was confirmed by ^{1}H, ^{13}C NMR and ESI-MS[16]. Yield: 1.53% (1.24 g). Yellow oil.

^{1}H NMR ($CDCl_3$, 500MHz) δ 11.71 (1H, s), 6.73 (1H, d, J=10 Hz), 6.23 (1H, s), 5.48 (1H, d, J=10 Hz), 5.06-5.12 (2H, m), 2.52 (3H, s), 2.02-2.13 (4H, m), 1.95 (2H, t, 8.3 Hz), 1.68-1.77 (1H, m), 1.67 (3H, s), 1.57-1.59 (6H, 2s), 1.40 (3H, s). ESI-MS: Exact-370.48 found- (M+1-18) = 353.46

2.4.5 Synthesis of daurichromenic acid derivatives and (-) hongoquercin A

2.4.5.1 Methyl ester of daurichromenic acid (2)

To a solution of Daurichromenic acid 1 (100 mg, 0.2699 mmol) in methanol (5 mL) and diethyl ether (5 mL) was added a solution of TMS-CH_2N_2 in hexane until the color of the solution became yellow at 0°C. The reaction mixture was stirred at same temperature for 0.5 h and at room temperature for 1 h. The reaction was quenched with acetic acid and concentrated under vacuum to afford a residue that was purified by silica gel column chromatography using hexane/ ethyl acetate (9.5:0.5) as an eluent to give the ester 2[17] with yield 97% . Colorless oil.

^{1}H NMR ($CDCl_3$, 500 MHz) δ 11.97 (1H, s), 6.72 (1H, d, 10 Hz), 6.18 (1H, s), 5.47 (1H, d, J=10.2 Hz), 5.05-5.11 (2H, m), 3.91 (3H, s), 2.45 (3H, s), 1.93-2.10 (6H, m) 2.97-3.00, 1.57-1.76 (2H, m), 1.66 (3H, s), 1.56-1.58 (6H, 2s), 1.39 (3H, s).

2.4.5.2 Methyl(S,E)-2-(4,8-dimethylnona-3,7-dien-1-yl)-5-methoxy-2,7-dimethyl-2H-chromene-6 carboxylate (3)

To a solution of 2 (59 mg, 0.16mmol) in DMF (3 mL) was added MeI (55 mg, 0.40 mmol) at room temperature. The reaction mixture was stirred at 90°C for overnight. After completion of the reaction, the reaction mixture was brought to room temperature and extracted with EtOAc. Organic layer was concentrated,

and residue was purified by silica gel column chromatography using hexane/ ethyl acetate (9:1) as an eluent to give the 3 with 59 mg (yield 94%). Colorless oil.

^{1}H NMR ($CDCl_3$, 500 MHz) δ 6.55 (1H, d, 10 Hz), 6.42 (1H, s), 5.56 (1H, d, J=10 Hz), 5.06-5.11(2H, m), 3.89 (3H, s), 3.78 (3H, s), 2.24 (3H, s), 1.94-2.05 (6H, m), 1.56-1.58 (2H, m), 1.67 (3H, s), 1.56-1.58 (6H, 2s), 1.38 (3H, s).

2.4.5.3 (S,E)-2-(4,8-dimethylnona-3,7-dien-1-yl)-5-methoxy-2,7-dimethyl-2H-chromene-6-carboxylic acid (4)

To a solution of 3 (50 mg, 0.13mmol) in MeOH (2 mL) and THF (2 mL) was added NaOH (6M, 2.5 mL) at room temperature. The reaction mixture was stirred at 100^o C for 1-2 h. After completion of the reaction, the reaction mixture was brought to room temperature, solvent was evaporated and neutralized with 2N HCl and extracted with EtOAc. Organic layer was concentrated, and residue was purified by silica gel column chromatography using hexane/ ethyl acetate (9.5:0.5) as an eluent to give the 4 with 59 mg (yield 83%). Colorless oil.

^{1}H NMR (CDCl3, 500 MHz) δ 10.50 (1H, s), 6.55 (1H, d, 10.2 Hz), 6.53 (1H, s), 5.63 (1H, d, J=9.2 Hz), 5.06-5.11(2H, m), 3.87 (3H, s), 2.50 (3H, s), 1.94-2.15 (6H, m) 2.97-3.00, 1.65-1.80 (2H, m), 1.67 (3H, s), 1.56-1.58 (6H, 2s), 1.41 (3H, s).

After obtaining DCA 1 as potent inhibitor of SMS by screening library of medicinal plants, SAR study was applied to identify the role of carboxylic acid and hydroxyl group towards SMS activity (Figure-1). Compound 2[17] was synthesized by methylating reagent TMS-CH_2N_2, which was turned out to be inactive derivative of DA. It gave a hint that carboxylic acid functional group is very important for SMS inhibition. To further confirm its role compounds 3 and 4 were synthesized, as we expected compound 4 with free carboxylic acid group turned out to be an inhibitor of SMS.

2.4.5.4 (–)-(5R,8S,10R)-9,15-didehydro hongoquercin A methyl ester (5)

To a solution of 2 (194 mg, 505 μmol) in fluorobenzene (10 mL) at room temperature was added ferric chloride ($FeCl_3$) (81 mg, 499 μmol) and stirred for 8 h until the disappearance of the starting material. After evaporation of fluorobenzene, to the residue was added 10 mL of water and extracted with ethyl acetate. The combined organic layer was dried with Na_2SO_4, and the residue was purified by silica gel column chromatography using 5% EtOAc in hexane, which yielded 5 as a white solid (46%). White solid.

^{1}H NMR ($CDCl_3$, 500 MHz) δ 11.99 (1H, s), 6.50 (1H, s), 6.19 (1H, s), 3.91 (3H, s), 2.45 (3H, s), 2.20 (1H, ddd, J = 3.5, 3.5, 13.0Hz), 2.05 (1H, d, J = 12.5Hz), 1.90 (1H, ddd, J = 4.5, 13.0, 13.0Hz), 1.80 (1H, d, J = 13.5Hz), 1.65–1.70 (1H, m), 1.58–1.62 (1H, m), 1.44 (3H, s), 1.41–1.52 (3H, m), 1.17 (3H, s), 1.09– 1.20 (2H, m), 0.92 (3H, s), 0.86 (3H, s); ^{13}C NMR (125MHz, CDCl3) δ 172.5, 159.5, 156.3, 148.8, 141.6, 111.4, 108.9, 108.3, 105.0, 79.2, 52.2, 41.5, 41.4, 39.3, 38.0, 33.6, 33.3, 26.9, 24.4, 23.5, 21.6, 19.3, 18.8; ESIMS m/z calcd for $C_{24}H_{33}O_4$ (M^++H) 384.5, found 385.1; $[\alpha]_D$ –176.1 (c 0.10, CHCl3); ECD (MeCN, λ [nm] ($\Delta\varepsilon$), c 0.466mM): 338 (+0.53), 299 (–6.08), 292sh (–5.73), 268sh (–1.42), 255 (–0.46), 236sh (–1.87), 225 (–3.87), < 200 (< –6.06).

2.4.5.5 (–)-(5R,8S,10R)-9,15-didehydro hongoquercin A (6).

To a solution of 5 (27.0 mg, 69.9 μmol) in methanol (1 mL) and THF (2 mL) was added 6M aq NaOH (1.5 mL) and refluxed for 2 h. The reaction mixture was then acidified with 2% aq HCl and extracted with CH_2Cl_2. The combined organic layer was washed with brine, dried over Na_2SO_4, and concentrated. The crude residue was purified by silica gel column chromatography using 20% EtOAc in hexane, which yielded 6[16] as a white solid(84%). White solid.

^{1}H NMR ($CDCl_3$, 500 MHz) δ 11.69 (1H, s), 6.50 (1H, s), 6.24 (1H, s), 2.53 (3H, s), 2.20 (1H, ddd, J = 3.5, 3.5, 13.0 Hz), 2.05 (1H, d, J = 12.5 Hz), 1.90 (1H, ddd, J = 4.5, 13.0, 13.0 Hz), 1.79 (1H, d, J = 13.5 Hz), 1.64–1.70 (1H, m), 1.56–1.61 (1H, m), 1.42 (3H, s), 1.37–1.51 (3H, m), 1.16 (3H, s), 1.08–1.20 (2H, m), 0.91 (3H, s), 0.86 (3H, s); ^{13}C NMR (125 MHz, $CDCl_3$) δ 176.4, 160.5, 157.5, 148.8, 143.4, 112.1, 108.9, 108.2, 103.7, 79.5, 52.2, 41.5, 39.3, 38.0, 33.6, 33.3, 27.1, 24.5, 23.5, 21.6, 19.3, 18.8; ESI-MS m/z calcd for $C_{23}H_{30}NaO_4$ (M^++Na) 393.5, found 393.3; $[\alpha]_D$ –164.6 (c 0.10, CHCl3); ECD (MeCN, λ [nm] ($\Delta\varepsilon$), c 0.421 mM): 335 (+0.54), 298 (–6.48), 290sh (–6.18), 270sh (–2.49), 256 (–1.10), 235sh (–2.36), 228 (–3.07), < 200 (<–7.27).

2.4.5.6 (-) hongoquercin A (7)

To a stirred solution of 6 (0.14 mmol) in EtOAc (10 ml) was added 10% Pd/C (0.028 mmol). The reaction mixture was stirred overnight at 40 °C under H_2 atmosphere. The solid was filtered off and the filtrate was concentrated under vacuum to afford a residue that was purified by silica gel column chromatography using hexane/EtOAc (8.0:2.0) to give 7 (74%) white solid. White solid.

^{1}H NMR (500 MHz, $CDCl_3$) δ 11.78 (1H, s), 6.14 (1H, s), 2.63 (1H, dd, J=16.8 Hz), 2.44 (3H, s), 2.19-2.25 (m, 1H), 2.01 (1H, dt, 3.1, 13.0 Hz), 1.69 (2H, m), 1.54-1.60 (3H, m), 1.48 (1H, dd, J= 5.4, 13.0 Hz), 1.38-1.43 (1H, m), 1.28-1.35 (2H, m), 1.13 (3H, s), 0.96 (1H, dd, J= 2.2, 12.4 Hz), 0.90 (1H, dd, J= 3.2, 13.0 Hz), 0.85 (3H, s), 0.83 (3H, s), 0.78 (3H, s). $[\alpha]_D$: +109.1 (c 1.00, $CHCl_3$).

2.4.6 SMS assay

Cell lysates were prepared as follows: ZS/SMS1 and ZS/SMS2 cells (protein concentration 0.1 μg/μL) were diluted by Tris-buffer (pH 7.5) 20 mM and sonicated. Aliquots of the cell lysates 100 μL were added 1 μL of inhibitor of

desired concentration and incubated at 37°C. After 30 min, the solutions were added 1 µL of C6-NBD-ceramide and incubated for 3 h at 37°C. The reaction was stopped by addition of 400 µL of MeOH/CHCl3 [1/2 (v/v)]; the mixture was shaken and centrifuged (1500 rpm x 5 min). The formation of C6-NBD-sphingomyelin was quantified by determination of the peak area of C6-NBDsphingomyelin using HPLC. A reverse phase HPLC assay using a JACSO HPLC system was developed for the quantitative analysis of the inhibitory activity. Figure 3 shows assay protocol of SMS.

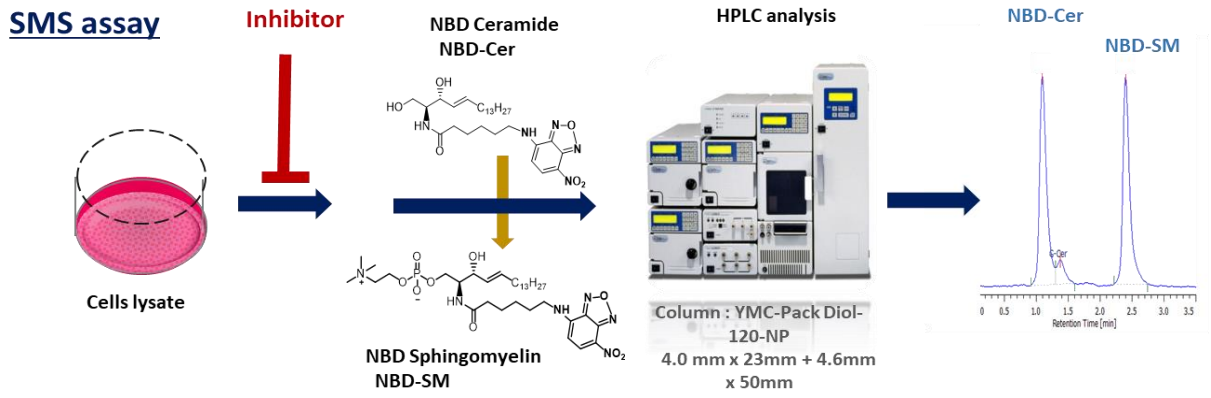

Figure 3: SMS assay protocol

The system was equipped with a PU-2089 Plus and FP-2020 Plus set at λex = 470 nm and λem = 530 nm. A 50 x 4.6 YMC-Pack Diol-120-NP column (5-µm particle size) was used with mobile phase (IPA/hexane/water) at a flow rate of 1.0 mL/min

2.4.7 Discussion

The multiple purification of Rhododendron dauricum leads to isolate daurichromenic acid a novel scaffold to inhibit SMS inhibition invitro. Leaves of Rhododendron dauricum is reported as anti-HIV and treating of many diseases and involved in cell proliferation, and as well as one of well-known practically

used Chinese traditional medicine. We synthesized seven derivatives of daurichromenic acid and in which (-) hongoquercin A turns out to be good inhibitor among derivatives still we couldn't manage to get best inhibitor molecule than DCA. Structures of isolated and All synthesized compounds were analyzed using Various spectroscopic methods such as UV, IR, HRMS and optical rotation for synthesized compounds. Our work, best to our knowledge, this is first time report on Daurichromenic acid and derivative of DCA, (-) hongoquercin A as SMS inhibitor.

2.5 Conclusions

In summary, to discover selective SMS inhibitors, screening of medicinal plants leads to isolate daurichromenic acid as potent SMS inhibitor. Along with synthesis of (-) hongoquercin A from daurichromenic acid, we have synthesized seven derivatives of daurichromenic acid and their inhibitory activities against purified SMS1 and SMS2 were evaluated, respectively. The results showed that DA derivatives exhibited significant potential in both potent towards SMS1 and SMS2. (-) hongoquercin A possessed higher activity than DCA, addition to daurichromenic acid (1), (-) hongoquercin A which turned out to be another novel SMS inhibitor, their efficacy *in vivo* needs to be explored. In conclusion, inhibitors of sphingomyelin synthase are viable therapeutic options with high untapped potential.

2.6 References

1. Hannun, Y. A. & Obeid, L. M. Sphingolipids and their metabolism in physiology and disease. *Nature Reviews Molecular Cell Biology* **19**, 175–191 (2018)
2. Mitsutake, S. *et al.* Dynamic modification of sphingomyelin in lipid microdomains controls development of obesity, fatty liver, and type 2 diabetes. *J. Biol. Chem.* (2011). doi:10.1074/jbc.M111.255646
3. Li, Z. et al. Reducing Plasma Membrane Sphingomyelin Increases Insulin Sensitivity. Mol. Cell. Biol. (2011). doi:10.1128/mcb.05893-11
4. Hsiao, J. H. T., Fu, Y. H., Hill, A. F., Halliday, G. M. & Kim, W. S. Elevation in Sphingomyelin Synthase Activity Is Associated with Increases in Amyloid-Beta Peptide Generation. PLoS One (2013). doi:10.1371/journal.pone.0074016
5. Hayashi, Y. et al. Sphingomyelin synthase 2, but not sphingomyelin synthase 1, is involved in HIV-1 envelope-mediated membrane fusion. J. Biol. Chem. (2014). doi:10.1074/jbc.M114.574285
6. Ohnishi, T. et al. Sphingomyelin synthase 2 deficiency inhibits the induction of murine colitis-associated colon cancer. FASEB J. (2017). doi:10.1096/fj.201601225RR
7. Taniguchi, M. & Okazaki, T. The role of sphingomyelin and sphingomyelin synthases in cell death, proliferation and migration - From cell and animal models to human disorders. Biochimica et Biophysica Acta - Molecular and Cell Biology of Lipids (2014). doi:10.1016/j.bbalip.2013.12.003
8. Jalencasa X & Mestres J. On the origins of drug polypharmacology, Med. Chem. Commun., 2013,4, 80-87
9. Newman, D. J., Cragg, G. M. & Snader, K. M. Natural products as sources of new drugs over the period 1981-2002. Journal of Natural Products (2003). doi:10.1021/np030096l

10. Swamy, M. M. M. et al. Structure-inspired design of a sphingolipid mimic sphingosine-1-phosphate receptor agonist from a naturally occurring sphingomyelin synthase inhibitor. Chem. Commun. (2018). doi:10.1039/c8cc05595e
11. Othman, M. A. et al. Malabaricone C as Natural Sphingomyelin Synthase Inhibitor against Diet-Induced Obesity and Its Lipid Metabolism in Mice. ACS Med. Chem. Lett. 10, 1154–1158 (2019).
12. Kashiwada, Y. et al. Isolation of rhododaurichromanic acid B and the anti-HIV principles rhododaurichromanic acid A and rhododaurichromenic acid from Rhododendron dauricum. Tetrahedron (2001). doi:10.1016/S0040-4020(0)01144-3
13. Lee, K. H. Discovery and development of natural product-derived chemotherapeutic agents based on a medicinal chemistry approach. Journal of Natural Products (2010). doi:10.1021/np900821e
14. Cao, Y., Chu, Q. & Ye, J. Chromatographic and electrophoretic methods for pharmaceutically active compounds in Rhododendron dauricum. J. Chromatogr. B Anal. Technol. Biomed. Life Sci. 812, 231–240 (2004).
15. Taura, F. et al. Daurichromenic acid-producing oxidocyclase in the young leaves of Rhododendron dauricum. Nat. Prod. Commun. 9, 1329–1332 (2014).
16. Mándi, A., Swamy, M. M. M., Taniguchi, T., Anetai, M. & Monde, K. Reducing Molecular Flexibility by Cyclization for Elucidation of Absolute Configuration by CD Calculations: Daurichromenic Acid. Chirality (2016). doi:10.1002/chir.22606
17. Liu, K. & Woggon, W. D. Enantioselective synthesis of daurichromenic acid and confluentin. European J. Org. Chem. (2010). doi:10.1002/ejoc.200901403

18. Roll, D. M., Manning, J. K. & Carter, G. T. Hongoquercins A and B, new sesquiterpenoid antibiotics: Isolation, structure elucidation, and antibacterial activity. J. Antibiot. (Tokyo). (1998). doi:10.7164/antibiotics.51.635

^{1}H NMR of Daurichromenic acid (**1**) and **2**

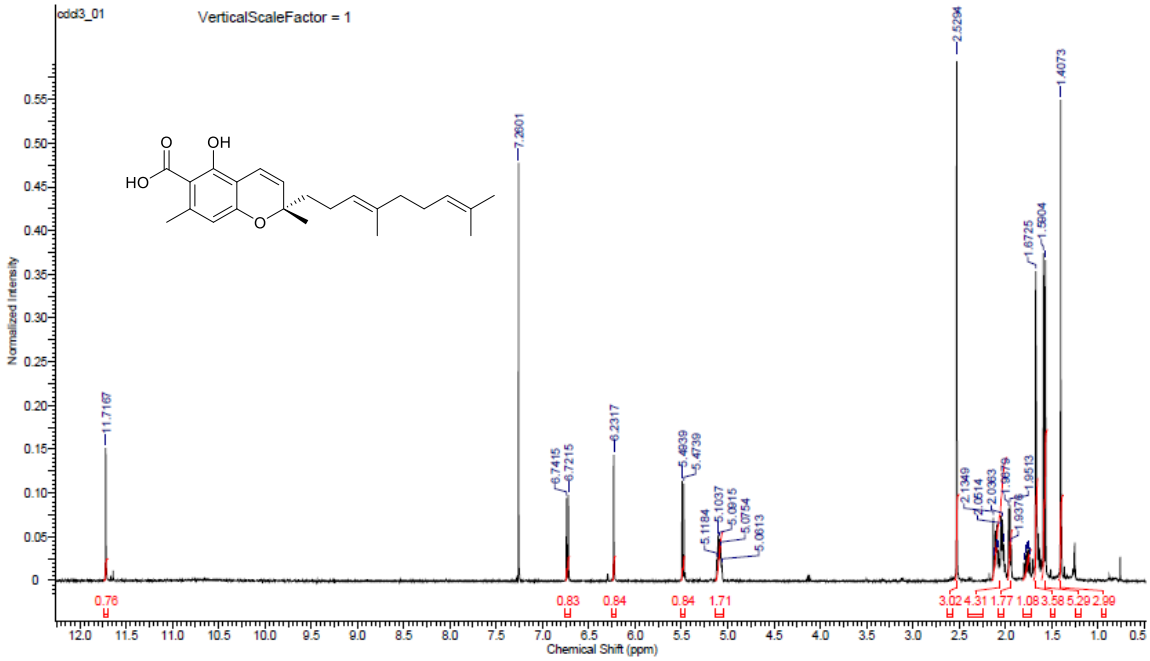

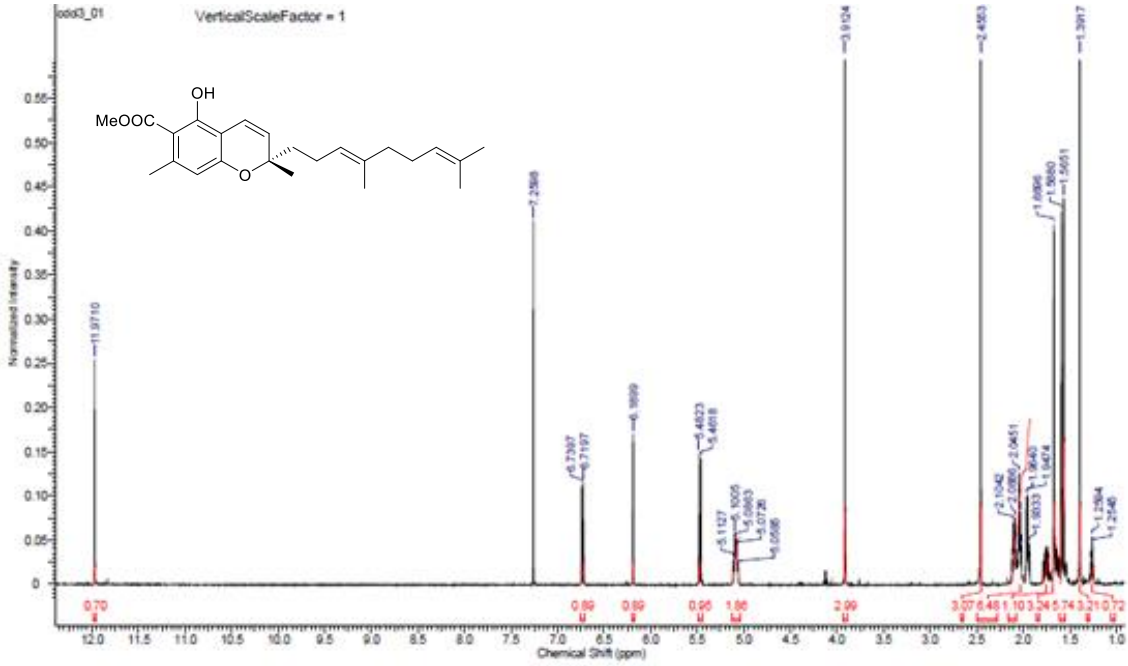

^{1}H NMR of **3** and **4**

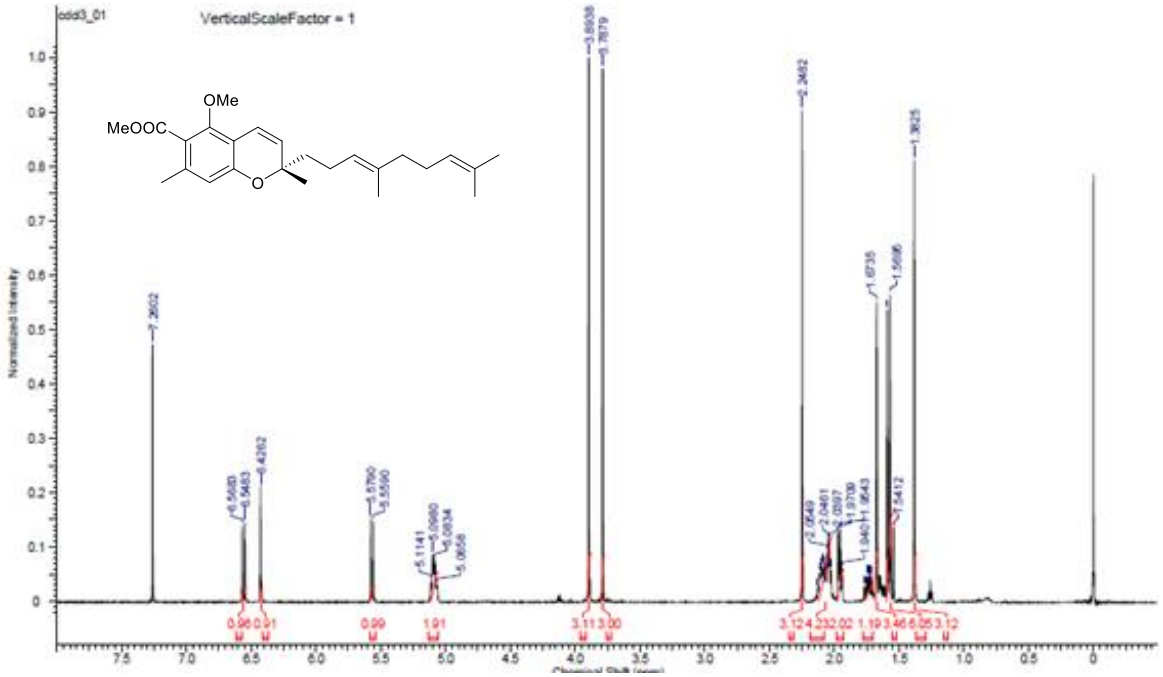

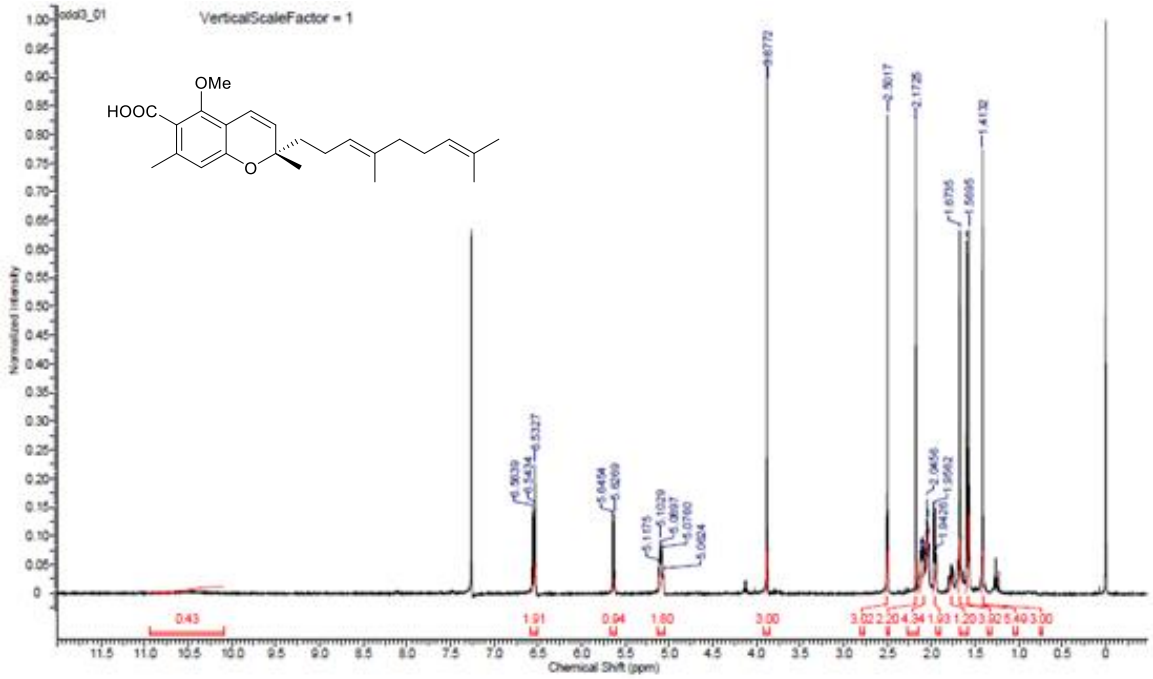

^{1}H NMR of **5** and **6**

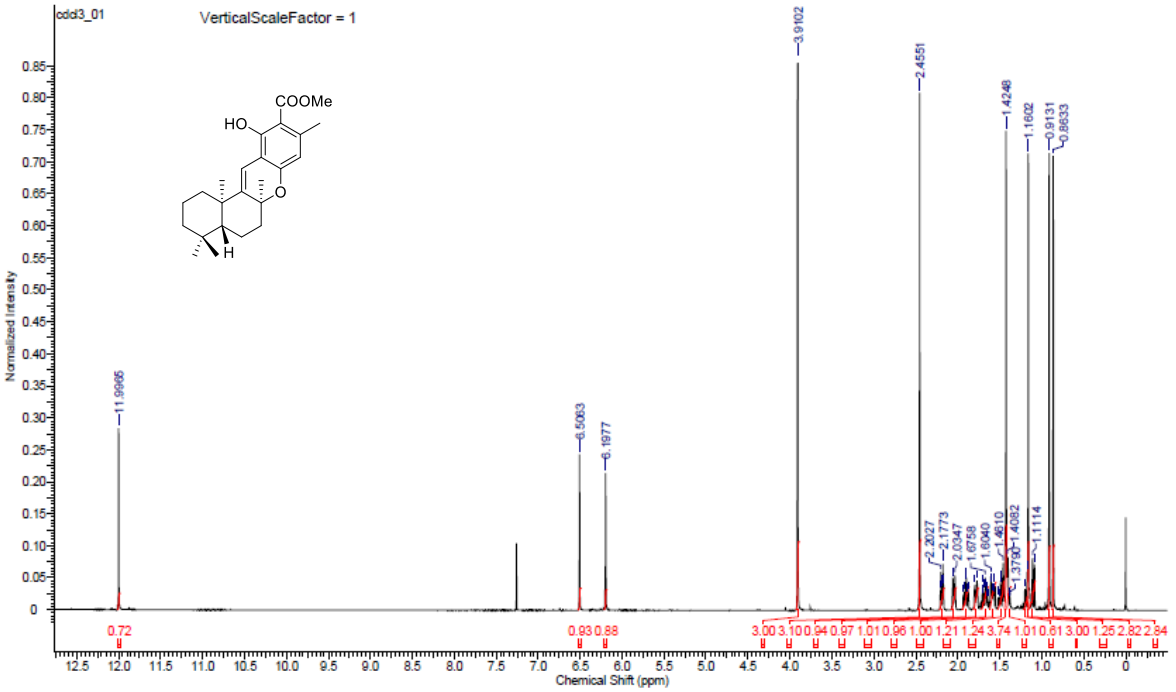

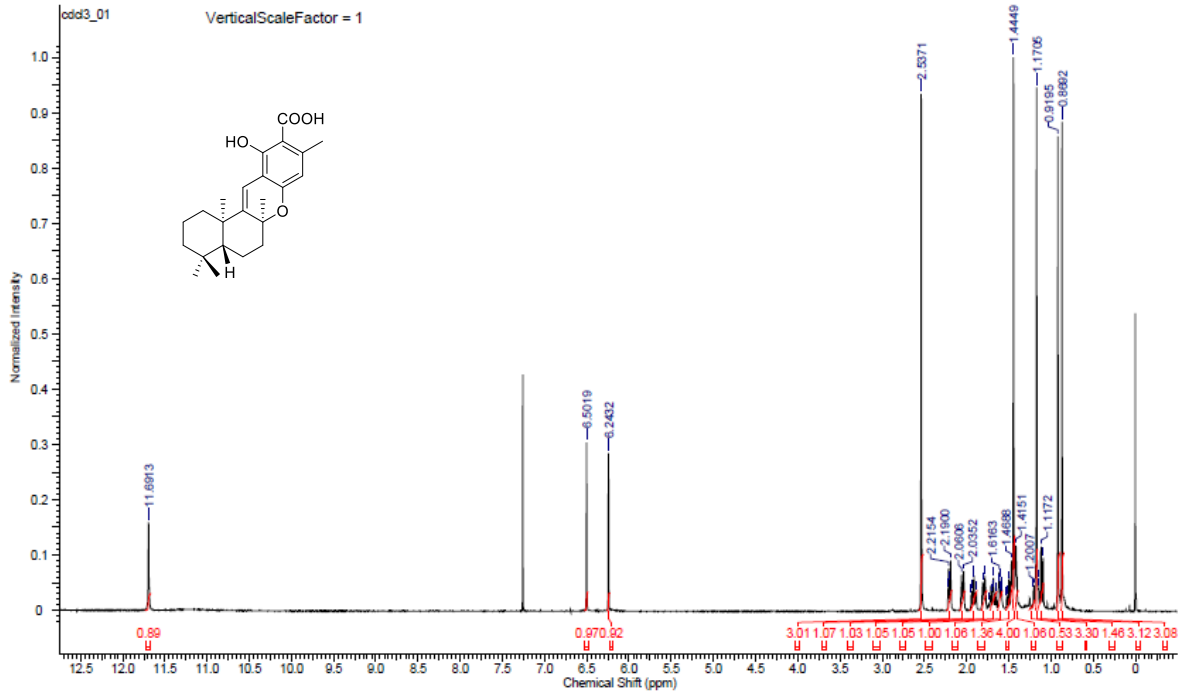

^{1}H NMR of (-) hongoquercin A (**7**)

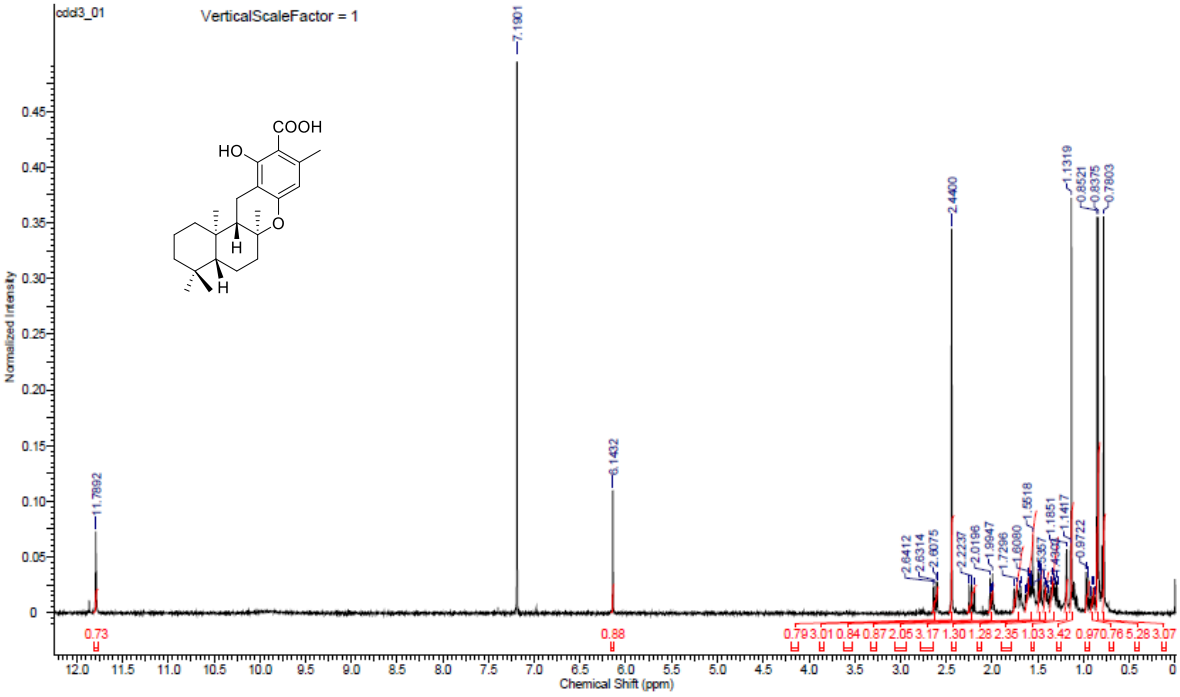

Chapter-3

Bio-guided isolation, derivative synthesis, and structure-activity relationships of daurichromenic acid, a novel scaffold as amyloid beta aggregation inhibitor

3.1 Abstract

Aggregation and misfolding amyloid beta peptides (Aβ) are pathological hallmark of Alzheimer's diseases. Contribution of Aβ leads to loss of cognitive function and progressive neuronal damage in central nervous system (CNS) in elderly people, thus discovery of new scaffold small molecule or natural plant extracts deserves much attention. We recently developed highly sensitive, rapid, automated high throughput screening method in search of Aβ aggregation inhibitors. To identify potential thereuptic agents, we screened methanol extracts derived from 504 Japanese medical plants for their Aβ aggregation inhibition by automated modified MSHTS assay system. Of these extracts, the leaves of Rhododendron dauricum was the most active in inhibiting amyloid beta aggregation inhibition at a concentration of 0.05 mg/ml using quantum Nano probe system. Bioguided fractionation of *Rhododendron dauricum* leaves lead to isolate a new scaffold potent anti- amyloid agent a meroterpenoid daurichromenic acid (57 μM). This is a first report on daurichromenic acid which detailed about inhibition of Aβ, apart from isolation we have also synthesized series of daurichromenic acid derivatives to evaluate its SAR studies. Among derivatives compound 4,5 and 13 were found to be potent amyloid aggregation inhibitor which reveal carboxylic acid group participation is very important to keep its inhibition activity.

3.2 Introduction

Amyloid aggregation and misfolding of proteins are commonly considered as the basis for multiple neuro degenerative diseases such as Alzheimer's diseases (AD), Parkinson disease, prion disease and Huntington disease[1] .AD is common form of dementia and its clinical manifestation characterized by progressive memory loss, visuospatial dysfunction, disorientation, behavioral turbulence, cognitive dysfunction and imbalances in lifestyle of elderly people particularly over 65-year-old [2,3]. At present AD is a 4th leading cause of death followed by heat disease, cancer and stroke worldwide, accounting 80% of cases and it is estimated to reach about 130 million by 2050 globally[4]. The most important pathological aspects of AD include changes of APP, phosphorylation of Tau, oxidative stress, among which production and subsequent aggregation of amyloid beta peptide(Aβ) called amyloid cascade hypothesis which is widely accepted. Aβ is formed after sequential cleavage of the amyloid precursor protein (APP), a transmembrane glycoprotein of undetermined function. APP can be cleaved by the proteolytic enzymes α-, β- and γ-secretase; Aβ protein is generated by successive action of the β and γ secretases (Figure 1)[5]. The brains of people with AD have an abundance of two abnormal structures like beta-amyloid plaques, which are dense deposits of protein and cellular material that accumulate outside and around nerve cells and neurofibrillary tangles, which are twisted fibers that build up inside the nerve cell

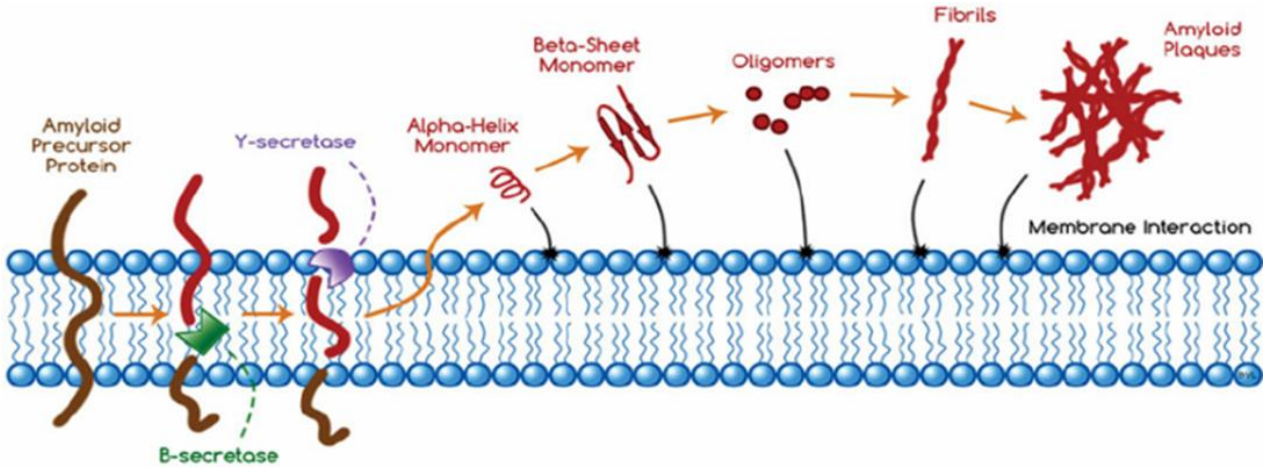

Figure 1: Formation of amyloid plaques

Deposition of abnormally aggregated amyloid beta (Aβ), a major component of extracellular senile plaques in the brain which is histological hallmark of AD [6] .Self-aggregation of isoform of Aβ (1-42) and Aβ (1-40) into amyloid fibers by a nucleation, condensation polymerization reported to be neurotoxic *in vitro* and *in vivo*[7] . However, many naturally occurring Aβ inhibitors have been limited for their practical usage due to their low effectiveness in interruption of Aβ production inhibition. . In this connection discovery and design of inhibitor for Aβ aggregation with new scaffold offers a promising threptic approach for prevention of AD.

Taken together, drugs with the potential Aβ aggregation inhibition or minimizing in Aβ production in AD pathogenesis are in demand. In this connection we screened 540 medicinal plant extracts which were grown wildly or cultivated in Hokkaido, Japan, to ascertain their activity against aggregation of Aβ inhibition. Aβ aggregation inhibition activity was evaluated by newly established method called the Microtiter scale -high -throughput screening (MSHTS) system. Using this new screening method, *Rhododendron dauricum* L. (RD, Ericaceae) was chosen for further investigation because the dried leaves are

used as crude drug having various biological activities and its availability from private gardens, but anti-Alzheimer's activity of *Rhododendron dauricum* is still unknown. In this connection bio-guided isolation lead to isolate daurichromenic acid from the dried leaves, a new scaffold inhibitor for Aβ aggregation inhibition. Apart from isolation we also focused on SAR studies of its synthesized three derivatives which may lead to develop new drugs for AD.

3.3 Result and discussion

3.3.1 Bioassay-Guided Isolation of Daurichromenic acid from R. *dauricum*

Recently Tokuraku group reported isolation of rosmarinic acid from *Satureja hortensis* (Family: Lamiaceae) by screening of 56 species by newly established Microtiter scale -high -throughput screening (MSHTS)[8] and its regarded as one of the strong Aβ aggregation inhibitor. To intend to search for novel scaffold inhibitor for Aβ aggregation, the modified (MSHTS) method[9,10] is used to screen 540 Hokkaido plant extracts to identify novel Aβ aggregation inhibitor. A well-known Chinese crude medicine *Rhododendron dauricum* (RD) was chosen based on Aβ aggregation assay results (MeOH extract EC_{50} :0.0160 mg/ml) and its bioavailability for further. Daurichromenic acid (DCA, EC_{50}: 57 μM) a meroterpenoid, was isolated from ether soluble fraction of methanolic extract of the fresh leaves of R. *dauricum* (Family: Ericaceae) by repeated chromatographic separation and purification over silica gel. (Figure 2) Structure was confirmed by ^{1}H, ^{13}C NMR and ESI-MS data. analysis as well as compared with previously

reported values[11]. ESI-MS showed m/z (M+1-18) = 353.46, suggesting the molecular formula of isolated compound $C_{23}H_{30}O_4$.

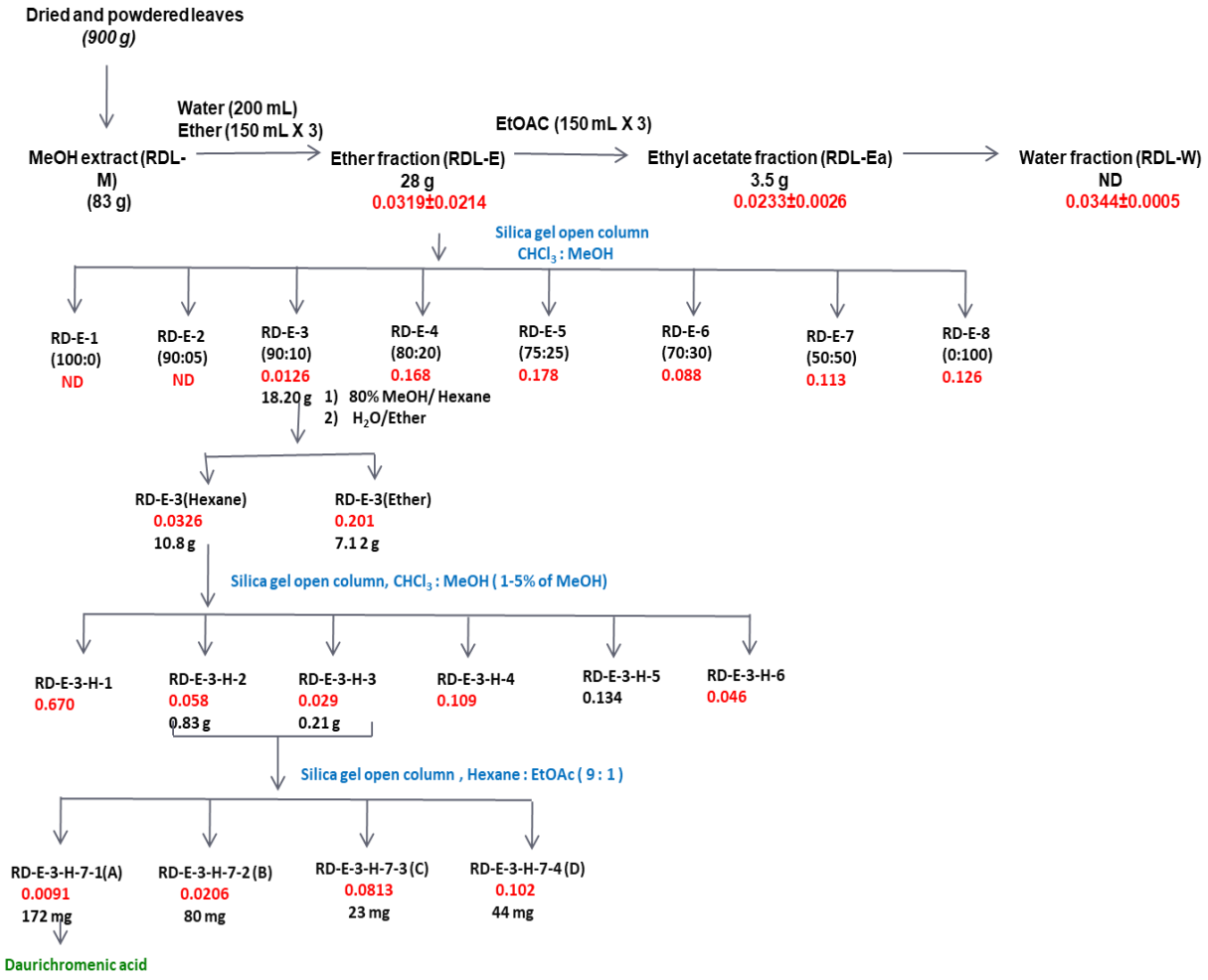

Figure 2 (A) Isolation of DCA from Rhododendron dauricum leaves (B) structure of DCA (1)

3.3.2 Synthesis of daurichromenic acid derivatives

SAR method is extensively used to optimize and develop various types of drugs. The in-silico methods developed using SAR include the statistical method, quantum analysis, artificial network modeling, validation method, etc. The toxicity of a drug is critically linked to its dose. If the dosage of a drug is too high, it can cause toxicity, and if it is too low, it can lead to no or less activity. Thus, the minimum effective concentration of a drug is a rather important property, and this parameter can also be determined using SAR. Also, the lack of specificity of a drug can also lead to side-effects. So, we decided to check functional group participation in DCA. We used same method (Synthesis of DCA and their derivatives, **chapter 2,** Figure 3) to synthesize DCA derivatives including (-) hongoquercin A.

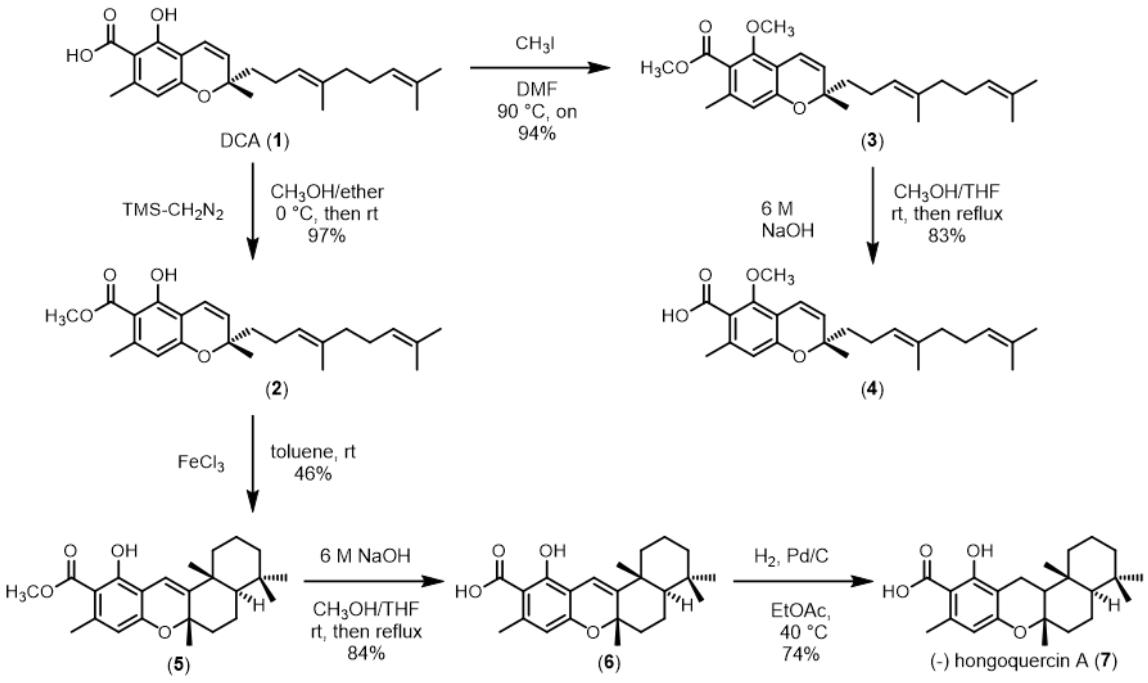

Scheme 1: Synthesis of DCA and its derivatives

DCA derivatives were synthesized. Compound (2) was prepared from DCA by selective methyl esterification of its carboxylic acid moiety by TMS-CH2N2.

Compound (3) was prepared by protecting the carboxylic acid and hydroxy groups with iodomethane, and compound (4) was prepared by hydrolysis of the methyl ester group of compound (3) Subsequently, hongoquercin A (7), which has been isolated from an unidentified terrestrial fungus[11] and exhibits antibacterial properties toward methicillin-resistant Staphylococcus aureus and vancomycin-resistant Enterococcus faecium [12,13]bwas prepared from compound (2). In the first step, compound (2) was treated with FeCl3 to obtain the cyclized derivative compound 5 (5). The methyl ester group of (5) was hydrolyzed to yield compound (6), and the double bond at the benzyl position of compound (6) was reduced by Pd/C and H2 to obtain hongoquercin A (7) in moderate yield (Scheme 1).

3.3.3 Measurement of Aβ aggregation

To evaluate whether the natural products or synthesized inhibitors can effectively inhibit aggregation of Aβ, we screened 540 plant extracts, synthesized derivatives using modified Microtiter scale -high -throughput screening (MSHTS) system[9]. The schematic representation of MSHTS assay is showed in (Figure 2)

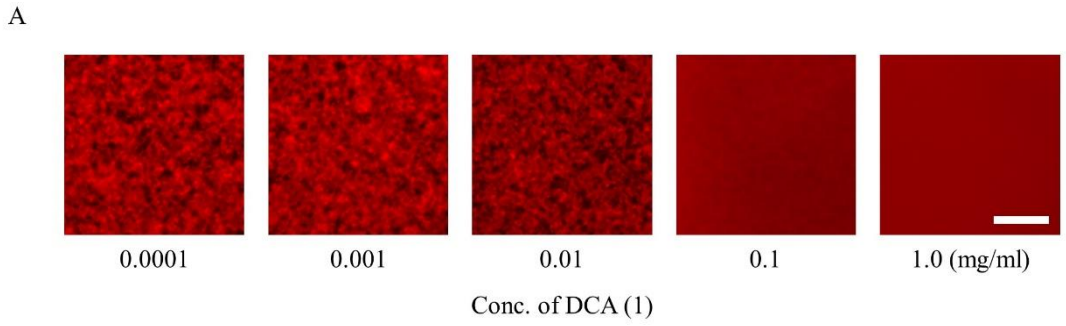

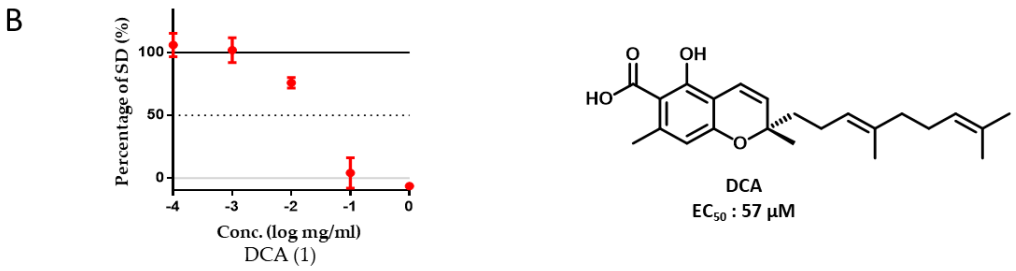

Figure 2: (A) Inhibition of Aβ aggregation by daurichromenic acid. 30µM QDAβ and 30µM Aβ were incubated with various concentrations of daurichromenic acid **(**B) Estimation of EC_{50} values from inhibition curve that are plotted percentage of SD of fluorescence intensities in the micrograph versus concentration of daurichromenic acid

3.3.4 Structural activity relationship studies of Daurichromenic acid derivatives

SAR has emerged as a great tool to understand and develop the chemical and physical properties of drugs. The structural information accorded by SAR can help in designing an organized approach to create drugs that have desired potency and specificity. To establish the contribution of each structural module to activity. After obtaining Daurichromenic acid (DCA) (1) as a potential inhibitor for amyloid beta aggregation, we went ahead with the structure activity relationship (SAR) studies to understand the role of functional groups toward its inhibition potency. DCA is terpenoid, consisting of a benzopyran moiety substituted with carboxylic acid, hydroxyl and an unsaturated hydrophobic chain. To understand the role of functional groups in inhibiting Aβ aggregation, first we introduced methyl group selectively. Daurichromenic ester (2) was obtained by using TMS Diazomethane, but (2) turned out to be an inactive ester. Further compound (3) was synthesized by introducing methyl group at phenolic-OH and carboxylic acid -OH using methyl iodide as a reagent, however

compound (3) too turned out be inactive. These observations imply that the carboxylic acid functionality is essential for Aβ aggregation inhibition. To confirm this hypothesis of us, we proceeded with the hydrolysis of (3) to give rise to compound (4), which consists of free carboxylic acid and methylated phenolic hydroxyl group. As expected, (4) with free carboxylic acid retained its potency of Aβ aggregation inhibition, thus strengthening our assumption. DCA could be converted into an antibacterial active agent (-) hongoquercin A[11] by UV irradiation[12] and under acidic condition. Our group recently reported the synthesis of hongoquercin A derivative, and its stereochemistry has been assigned by circular dichroism spectroscopy. Similarly, we decided to convert methyl ester of DCA (2) into methyl ester of (-) hongoquercin A (7) by cycloaddition using Lewis acid ($FeCl_3$) to elaborate our SAR studies in a quest to obtain an Aβ inhibitor of different scaffold. We assumed that DCA carboxylic acid functional group in hongoquercin A derivative also might be essential for inhibitory activity as that of natural DCA. As expected, the compound (6) was inactive due to the protected carboxylic acid like compound (2). Alkaline hydrolysis of (6) gave rise to free carboxylic acid derivative of Hongoquercin A derivative (7), which inhibited Aβ aggregation (Figure 3).

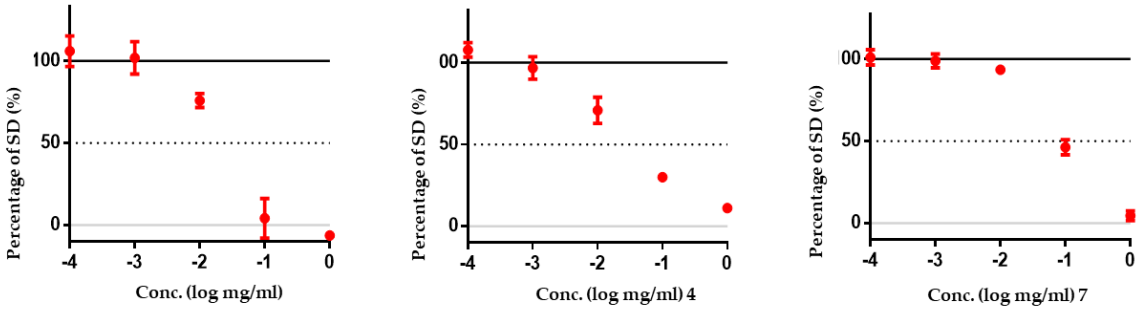

DCA 1 Compound 4 (-) hongoquercin 7 (238 µM)

Figure 3: Estimation of EC_{50} values from inhibition curve that are plotted percentage of SD of fluorescence intensities in the micrograph versus concentration of daurichromenic acid and its derivatives.

As a result of SAR studies, it could be asserted that the carboxylic acid in DCA and (-) hongoquercin A, derivative has a significant role in Aβ aggregation inhibition.

3.4 Experimental section

3.4.1 Materials and methods:

3.4.1.1 General.

The 1H NMR (500 MHz), ^{13}C NMR (125 MHz), spectra were recorded on a Bruker AV 500 spectrometer in chloform-*d*, using TMS as internal standard. ESI-MS spectra were recorded on a JASCO. Melting points were measured on a Micro Melting Point Apparatus, Yanaco Co., Ltd. Silica gel for column chromatography (CC), TLC plates: Silica gel 60 F_{254} (Merck), developed with $CHCl_3$: MeOH: H2O (65:35:10, lower phase), sprayed with a mixture of 5% ammonium molybdate and 1% cerium (IV) sulphate in 3.6N H_2SO_4 (Hanessian stain solution), or detected with UV lamp (UVGL-58 handheld at 254 nm).

3.4.1.2 Plant collection:

Five hundred and four plants grown wildly or cultivated in Hokkaido were collected from June to November 2004. Each was washed briefly, cut in small pieces using pruning shears and dried by hot air at 50 °C for 24 hours. Each dried material was powdered using mixer before solvent extraction. Twenty grams of dried and powdered material were extracted with 200 ml of methanol at room temperature for 24 hours. After filtration, the methanol solution was concentrated under reduced pressure to give residue. Each crude extract was

transferred to 30 ml of brown glass bottle and stored in refrigerator at -20 °C. Average yields based on each dry weight were about 25%. Each extract was dissolved in DMSO in a concentration of 100 mg/ml and the solution was stored in refrigerator at -20 °C. A part of each DMSO solution was used for several bioassay.

3.4.1.3 Screening of plant extracts using MSHTS method

Extraction, Isolation

The dried leaves (900 g) of *R. dauricum* were extracted with MeOH (3L × 3) at room temperature three times for 24 hours each. After exhaustive extraction, the combined MeOH solution was concentrated under reduced pressure to give a dark green residue of 83 g (9.2 % based on dry weight of leaves). Crude extract was suspended in H_2O (200 mL) and partitioned with ether (200 mL × 3), ethyl acetate (200 mL × 3) successively. After complete removal of each solvent by evaporation, ether, ethyl acetate and water fractions (28 g, 3.5 g and ND, respectively) were subjected to amyloid beta aggregation bioassay. We found out that ether fraction (28 g) and ethyl acetate fraction (3.5 g) showed good inhibition activity (0.0319±0.024 and 0.0233±0.0026 mg/mL, respectively). The active ether extract (28 g) was subjected to silica gel column chromatography and eluted with increasing polarity using mixture of $CHCl_3$/MeOH to give 8 fractions (F1-F8). The most active fraction ($CHCl_3$/MeOH =90 : 10 eluates, F3, 18.2g) was dissolved in 80% MeOH in water (500 mL) and extracted with hexane (200 mL × 3) to remove large amount of pigments. The aqueous MeOH solution was evaporated to about 100mL and then extracted with ether (200 mL × 3). From bioassay experiment, the hexane fraction was more active than ether fraction. The hexane fraction (10.8 g) was further fractionated by repeated silica gel column chromatography's guided by bioassay. The active component was isolated as colorless oil (172mg,

0.013%) and was identified as daurichromenic acid (15:1) (Fig.1) which was confirmed by spectroscopic published literature data.

Structure of Daurichromenic acid; yellow oil; ^{1}H NMR ($CDCl_3$, 500MHz) δ 11.71 (1H, s), 6.73 (1H, d, J=10 Hz), 6.23 (1H, s), 5.48 (1H, d, J=10 Hz), 5.06-5.12 (2H, m), 2.52 (3H, s), 2.02-2.13 (4H, m), 1.95 (2H, t, 8.3 Hz), 1.68-1.77 (1H, m), 1.67 (3H, s), 1.57-1.59 (6H, 2s), 1.40 (3H, s). ESI-MS: Exact-370.48 found- (M+1-18) = 353.46

3.4.1.4 Aβ aggregation inhibition assay.

Automated MSHTS system–sample preparation and mixing with Aβ[8,9]

Sample preparation was carried out using Automated Workstation JANUS G3 (Perkin Elmer). To make dilution series of samples, dilution buffer (10%EtOH, 1×PBS) was aspirated (Asp. Speed: 20 µl/s) using conductive chip that can detect liquid level and injected (Dsp. Height: 0.75 mm, Dsp. Speed: 10 µl/s) into each well of 384-well plate (384 Hard-shell micro plate HSP3951, BIO-RAD) without wells for injecting stock sample solution. Stock sample solutions were prepared and were injected manually into the vacant wells of the 384-well plate. As a control without any inhibitor, dilution buffer alone was injected into the well instead of stock sample solution. The stock sample solution or control solution was aspirated (Asp. Height: 2 mm, Asp. Speed: 10 µl/s), injected (Dsp. Height: 4 mm, Dsp. Speed: 10 µl/s) into the next well containing the dilution buffer and mixed by pipetting (Asp. Height: 2 mm, Dsp. Height: 4 mm, mix speed: 25 µl/s, Mix Cycles: 5). This dilution step was repeated 5 times, so that 6 dilution series can be prepared for each sample. The diluted samples in the 384-well plate were aspirated using 384-chip head (Asp. Height: 1 mm, Asp. Speed: 3 µl/s) and injected (quadruplicate) (Dsp. Height: 1 mm, Dsp. Speed: 10 µl/s) into a 1536-well plate (1536 well FIA black plate, Greiner Bio-One) at 2.5 µl per well. The Aβ

solution, which is a mixture of 50 nM QDAβ and 50 μM Aβ42, was prepared in microcentrifuge tube at 4 °C, aspirated (Asp. Speed: 30 μl/s) using conductive chip that can detect liquid level, and injected (Dsp. Height: 0.5 mm, Dsp. Speed: 20 μl/s) into the cold 384-well plate at 4 °C. Finally, 2.5 μl of the Aβ solution were aspirated (Asp. Height: 1 mm, Asp. Speed: 3 μl/s) from the 384-well plate using 384-chip head, injected (Dsp. Height: 0.5 mm, Dsp. Speed: 10 μl/s) into the 1536-well plate containing diluted samples and mixed by 3-times pipetting (Mix height: 0.5 mm, Mix speed: 50 μl/s, Mix volume: 3.5 μl, Mix Cycles: 3). The 1536-well plate was sealed up using a plate seal (T-2417-8, BM Bio) to prevent evaporation. In order to remove bubbles and flatten the liquid surface, the 1536 well plate centrifuged at 1,530 xg for 5 min by a multi-well plate centrifuge.

Aggregation activity on Aβ of plant extracts, fractions, Daurichromenic acid and synthesized derivatives was measured by modified MSHTS system (). Notably, EC_{50} values were investigated by various concentration of extracts Daurichromenic acid and their derivatives, Co-incubation of 30 nM QD-labeled Aβ (QDAβ), and 30 μM Aβ in PBS containing 5% EtOH and 3% DMSO at 37°C for 24 h in 1536-well plate (782096, Greiner) to form QDAβ-Aβ aggregates. Color CCD camera equipped (DP72, Olympus) Inverted fluorescence microscope (Nikon, TE2000) is used to observe center of each well. ImageJ software (NIH) is used to measure central region of each well in a plates to rectify standard deviation (SD) values of fluorescence intensities which is of 10,000 pixels (100 × 100 pixels: 167 × 167 μm) .The SD values, which were approximately proportional to the amount of aggregates[10] were plotted against the inhibition concentrations of added plant extracts and synthesized daurichromenic acid derivatives to show an inhibition curve.

Automated MSHTS system–Imaging and Data analysis

After centrifugation by a multi-well plate centrifuge, the 1536 well plate was observed by an inverted fluorescence microscope system (ECLIPSE Ti-E, Nikon) equipped with a color CCD camera (DS-Ri2, Nikon). QD was imaged using a 4 × objective lens and a TRITC filter set (TRITC-A-Basic-NTE, Semrock). The images of each well were captured using auto exposure up to 160 ms and then raise the camera gain to 32x. At that time, the target maximum light intensity of the camera setting was set to 50%, and the size of the region of interest (ROI) was set to 432 x 432 pixel of the center of each well. To focus on all wells of 1536 well plate, we used XYZ Overview program of NIS elements (Nikon) or Perfect Focus System (Nikon). The 1536 well plate was incubated at 37 °C for 1 day and observed under the same conditions as above. SD value of the fluorescence intensity of each pixel was measured by General Analysis program of NIS-Elements (Nikon). The half-maximal effective concentration (EC_{50}) was estimated from the SD values by Prism software (GraphPad) using an EC_{50} shift by global fitting (Asymmetric sigmoidal, 5 parameters logistic) according to our previous method[10]

Statistical analysis

Statistical analysis was performed using GraphPad curve for estimate the half maximal effective concentration (EC50) anti-Aβ. Aggregation. Significant differences between means at a level of 0.05 ($p < 0.05$) were considered significant**.**

3.5 Conclusions

In summary, our results demonstrated that bioassay guided isolation from *Rhododendron dauricum*, lead to daurichromenic acid, a new scaffold natural inhibitor for amyloid beta aggregation. SAR studies identified a new natural

product scaffold, (-) hongoquercin A, a derivative as a novel amyloid beta aggregation inhibitor.

3.6 References

1. Haass C, Selkoe DJ. Cellular processing of beta-amyloid precursor protein and the genesis of amyloid beta-peptide. *Cell* 1993; 75: 1039–42.

2. Glenner GG, Wong CW. Alzheimer's disease: initial report of the purification and characterization of a novel cerebrovascular amyloid protein. *Biochem Biophys Res Commun* 2012; 425: 534–9.

3. Bloom GS. Amyloid-beta and tau: the trigger and bullet in Alzheimer disease pathogenesis. *JAMA Neurol* 2014; 71: 505–8

4. Selkoe DJ, Hardy J. The amyloid hypothesis of Alzheimer's disease at 25 years. *EMBO Mol Med* 2016; 8: 595–608

5. Drolle E, Hane F, Lee B, Leonenko Z. Atomic force microscopy to study molecular mechanisms of amyloid fibril formation and toxicity in Alzheimer's disease. *Drug Metab Rev*. 2014;46(2):207-223.

6. Deba F, Peterson S, Hamouda AK. An Animal Model to Test Reversal of Cognitive Decline Associated with Beta-Amyloid Pathologies. *Methods Mol Biol.* 2019; 2011:393-412.

7. De-Paula VJ, Radanovic M, Diniz BS, Forlenza OV. Alzheimer's disease. *Subcell Biochem*. 2012; 65:329-352.

8. Ogara, T., Takahashi, T., Yasui, H., Uwai, K., & Tokuraku, K.. Evaluation of the effects of amyloid β aggregation from seaweed extracts by a microliter-scale high-throughput screening system with a quantum dot nanoprobe. *Journal of bioscience and bioengineering*, 2015, 120, 45–50.

9. Tokuraku, K., Marquardt, M., & Ikezu, T. (2009). Real-time imaging and quantification of amyloid-beta peptide aggregates by novel quantum-dot nanoprobes. *PloS one*, *4*, 12, e8492.

10. Ishigaki, Y., Tanaka, H., Akama, H., Ogara, T., Uwai, K., & Tokuraku, K. (2013). A microliter-scale high-throughput screening system with quantum-dot nanoprobes for amyloid-β aggregation inhibitors. *PloS one*, 8, 8, e72992.

11. Mándi, A., Swamy, M. M. M., Taniguchi, T., Anetai, M. & Monde, K. Reducing Molecular Flexibility by Cyclization for Elucidation of Absolute Configuration by CD Calculations: Daurichromenic Acid. *Chirality*, 2016.

12. Liu, K. & Woggon, W. D. Enantioselective synthesis of daurichromenic acid and confluentin. *European J. Org. Chem.* ,2010.

13. Roll, D. M., Manning, J. K. & Carter, G. T. Hongoquercins A and B, new sesquiterpenoid antibiotics: Isolation, structure elucidation, and antibacterial activity. *J. Antibiot.* (Tokyo). 1998.

Overview of research

Drug design is the inventive process of finding new medications based on the knowledge of the biological target. The notion of 'one molecule – one target – one disease' has been a prevalent paradigm in pharmaceutical industry. The main idea of this approach is the identification of a single protein target whose inhibition leads to a successful treatment of the examined disease.

Modulation of the activity of a specific enzyme or receptor by a small molecule is one of the cornerstones of modern target-based drug discovery. However, small molecules frequently bind to multiple target molecules, influencing both drug efficacy and safety. Although the one-drug-hits-one target approach was dominant in the post-genomic era, it is regarded as inadequate to address

complex diseases. The multitarget approach has become a fruitful area of drug discovery, particularly in developing medicines to treat major complex diseases. For example, natural products such as genistein, curcumin, and tashinone have been reported to inhibit amyloid β (Aβ) and human islet amylin (hIAPP) associated with type 2 diabetes. Another compound, miltirone, isolated from *Salvia miltiorrhiza*, was shown to be a dual inhibitor of P-glycoprotein and cell growth in doxorubicin-resistant HepG2 cells.

From our current study we successfully isolated daurichromenic acid (1), as a potent dual inhibitor for sphingomyelin synthase (SMS) and amyloid beta (Aβ) aggregation inhibition (Figure 1).

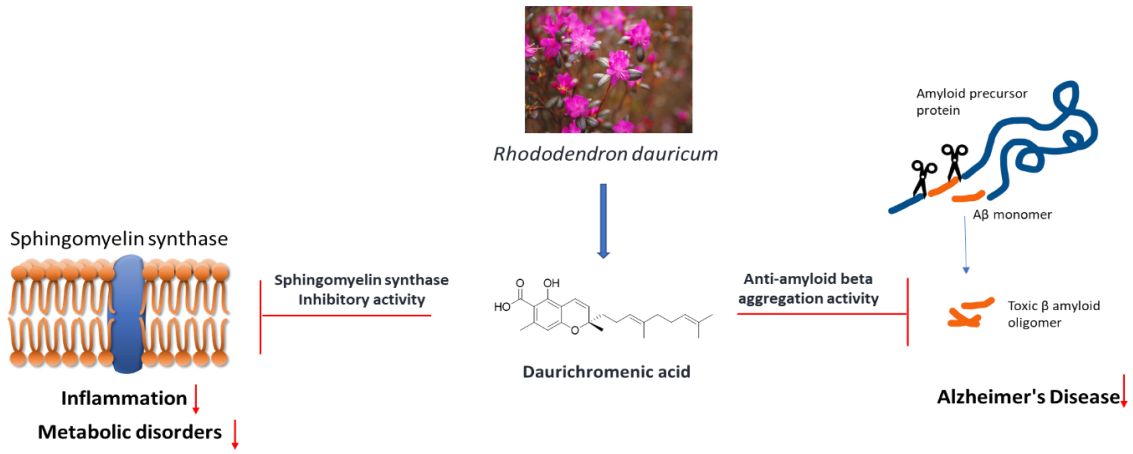

Figure 1: Dual inhibitor for SMS and Aβ aggregation inhibition from *Rhododendron dauricum*

To determine the biological properties of DCA and its derivatives and whether they are promising candidate drugs, the ability of these compounds to inhibit SMS activity was analyzed, as was the structure–activity relationship of these compounds in cell-based SMS assays. Furthermore, the effects of DCAs and natural SMS inhibitors on Aβ aggregation were assessed by microtiter-scale high-

throughput screening (MSHTS) assays.

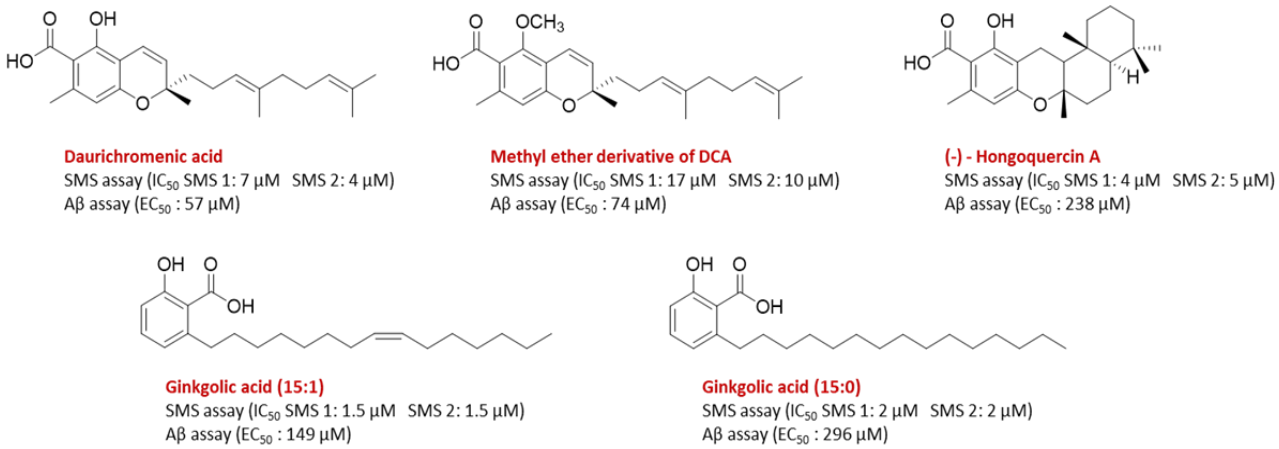

Figure 2: Dual inhibitors of SMS and Aβ aggregation

The present study showed that DCA, a terpenoid from the leaves of *Rhododendron dauricum*, is a natural inhibitor of sphingomyelin synthase. Few of its derivatives, including compounds 4, and (-) hongoquercin A, also showed good inhibitory activity against SMS. In addition, similar three compounds were found to inhibit $A\beta_{42}$ aggregation (Figure 2). Compounds with SMS inhibition properties against cell-lysate assays and the fluorescent substrate C6-NBD (4-nitrobenzo-2-oxa-1,3-diazole)-Cer share a carboxylic acid moiety which is also related to anti-aggregative properties against amyloid beta protein. MSHTS assays were used to evaluate amyloid beta aggregation activity using DCA and their derivatives. DCA (1) and compound 4 and (-) hongoquercin A with the presence of a carboxylic acid group tend to inhibit both SMS and Aβ aggregation inhibition. Our work, to the best of our knowledge, is the first report on daurichromenic acid and derivatives of DCA and compound 4 and (-) hongoquercin A as a dual inhibitor for sphingomyelin synthase and amyloid beta aggregation.

Acknowledgements

This doctoral thesis would not have been possible without the support of many people.

Firstly, I wish to express my gratitude to my supervisor Professor Kenji Monde, who was generously, abundantly, and consistently encouraging and offered irreplaceable guidance throughout the course of this research. There is no doubt that this research could not be completed without his constant and wise encouragement. I also wish to express my thanks to Professor Masaki Anetai for his valuable guidance and time towards my PhD journey. He contributed to my research and involved in valuable discussion for solving my experimental issues and supporting me in many ways.

My special thanks to my associate supervisors Prof. Shin-Ichiro Nishimura and Prof. Makato Demura and Prof Hiroshi Hinou for their valuable suggestions and inputs for progress of my research. Also, very special thanks to Dr Yuta Murai and Dr. Tohru Taniguchi for his invaluable advice and feedback on my research and for always being so supportive of my work.

I am also thankful to Associate professor Kiyotaka Tokuraku, and Associate professor Koji Uwai and Dr. Masahiro Kuragano for contributed to my research and involved in valuable discussion.

I am also hugely appreciative to Ms. Asano, Ms. Keiko Abe, Ms. Yoshiko Suga and Ms. Ogura for their valuable assistance and support especially in the administrative work.

Furthermore, I wish to thank my lab mates and colleagues at Monde laboratory, Hokkaido university which have provided a highly enriching experience during my studies and upheld the Hokkaido university value of collegiality and

community-building ‘throughout the years. Outside the Hokkaido university community, I must acknowledge the encouragement from a wide range of acquaintances over the years; many of which are scattered across the globe working to enrich the collective life of society.

I would also like to express my gratitude to MEXT for their financial support and IGP for giving this opportunity. This work would not have been completed without their financial support.

Moreover, I am deeply appreciative of the loyal support from a smaller circle of true friends who have stood shoulder-to-shoulder with me throughout various developments and exemplified excellence in various aspects of life. Lastly, I would like to thank my parents whom been unconditionally supportive and infinitely trusting throughout the successive stages of my life.

Publications

Papers (related to Doctoral Dissertation)

Hadya Virupaksha Deepak, Mahadeva M. M. Swamy, Yuta Murai, Yoshiko Suga, Masaki Anetai, Takuro Yo, Masahiro Kuragano, Koji Uwai, Kiyotaka Tokuraku, Kenji Monde. Daurichromenic acid from the Chinese traditional medicinal plant *Rhododendron dauricum* inhibits sphingomyelin synthase and Aβ aggregation. *Molecules*. 2020, **25**, 4077.

Rina Sasaki, Reina Tainaka, Yuichi Ando, Yurika Hashi, **Hadya Virupaksha Deepak**, Yoshiko Suga, Yuta Murai, Masaki Anetai, Kenji Monde, Kiminori Ohta, Ikuko Ito, Haruhisa Kikuchi, Yoshiteru Oshima, Yasuyuki Endo, Hitomi Nakao, Masafumi Sakono, Koji Uwai & Kiyotaka Tokuraku "An automated microliter-scale high-throughput screening system (MSHTS) for real-time monitoring of protein aggregation using quantum-dot nanoprobes" *Sci. Rep*, 2019, **9**, 2587